Supplement of Atmos. Chem. Phys., 25, 2763–2780, 2025
https://doi.org/10.5194/acp-25-2763-2025-supplement

Atmospheric Chemistry and Physics
Open Access
EGU

Supplement of

The critical role of aqueous-phase processes in aromatic-derived nitrogen-containing organic aerosol formation in cities with different energy consumption patterns

Yi-Jia Ma et al.

Correspondence to: Yu Xu (xuyu360@sjtu.edu.cn)

Table of Contents

Sect. S1. UPLC-ESI-QToFMS Analysis

The samples were analyzed using an Acquity UPLC coupled to a Xevo G2-XS QToF-MS (Waters), which is equipped with an electrospray ionization (ESI) source. The instrument offers a mass resolving power of ≥ 40 000 at full width at half maximum (FWHM) (m/z 956) (Wang et al., 2021b; Wang et al., 2021c). This high resolution ensures precise determination of molecular formulas. Data acquisition and processing were performed using MassLynx version 4.2 software. A mass tolerance of 5 ppm was applied to calculate potential molecular formulas for each detected ion. Instrument calibration was performed prior to each analysis to ensure the accuracy and reliability of the measurements.

Compounds with identical molecular formulas were summed without distinguishing isomers, as isomer differentiation based on retention time or fragmentation spectra is beyond the scope of this study. This approach aligns with recent studies using Fourier transform-ion cyclotron resonance mass spectrometry (FT-ICR MS) (Sun et al., 2024; Jiang et al., 2023; Su et al., 2021). The observed molecular formulas reflect the cumulative sum of isomeric species, as this method cannot differentiate them. The detected compounds ranged from m/z 50 to 700 (Ma et al., 2024; Ungeheuer et al., 2021; Praplan et al., 2014), covering small organic acids to larger secondary organic aerosol components. This range was well within the instrument's capabilities.

The addition of formic acid to the mobile phase played a crucial role in achieving optimal chromatographic separation and enhancing ionization efficiency during ESI–

MS analysis (Núñez and Paolo, 2014; Kuehnbaum and Britz-McKibbin, 2013). This approach is widely employed in the analysis of atmospheric organic compounds (Zhang et al., 2024; Abudumutailifu et al., 2024; Wang et al., 2021a). Although the acidic conditions introduced by formic acid may affect certain CHON compounds through hydrolysis or acid-catalyzed reactions, the aerosols analyzed in this study were generally acidic or mildly acidic (average pH values of 3–5). Additionally, the short elution time (18 minutes) minimized the likelihood of significant chemical changes to the compounds.

Sect. S2. Parameter calculation and compound classification

The concentrations of non-sea-salt (nss) Cl^- and K^+ were estimated using the following equation, based on Ni et al. (2013).

$$[\text{nss-X}] = [\text{X}] - [\text{Na}^+] \times a \quad \text{(S1)}$$

Here, [X] represents the concentrations of Cl^- and K^+, and *a* represents the typical ratio of the species to Na^+ in seawater, where ($[Cl^-]/[Na^+] = 1.80$ and $[K^+]/[Na^+] = 0.036$).

The double-bond equivalent (DBE) indicates the number of rings and double bonds in a molecule (Lechtenfeld et al., 2014; Bae et al., 2011). It was calculated as follows:

$$\text{DBE} = (2N_C + 2 - N_H + N_N) / 2 \quad \text{(S2)}$$

Here, N_C, N_H, and N_N denote the numbers of carbon (C), hydrogen (H), and nitrogen (N) atoms, respectively.

The carbon oxidation state (OS_C) is a key indicator of the compositional evolution of oxidized organic compounds (Kroll et al., 2011). It was calculated as follows:

$$OS_C \approx 2 \times N_O/N_C - N_H/N_C \quad \text{(S3)}$$

Here, N_C, N_H, and N_O refer to the numbers of carbon, hydrogen, and oxygen atoms in a molecule, respectively.

The modified aromaticity index (AI_{mod}) aids in identifying and characterizing aromatic-like compounds in aerosols (Xu et al., 2023; Zhong et al., 2023). It was calculated as follows:

$$AI_{mod} = (1 + N_C - 0.5 \times N_O - N_S - 0.5 \times N_N - 0.5 \times N_H) / (N_C - 0.5 \times N_O - N_S - N_N) \quad \text{(S4)}$$

Here, N_C, N_H, N_O, N_N and N_S represent the numbers of carbon, hydrogen, oxygen, nitrogen, and sulfur atoms in the molecular formula, respectively.

The van Krevelen diagrams and AI_{mod} values are widely used to classify organic compounds into specific categories (Xu et al., 2023; Su et al., 2021; Seidel et al., 2014). Based on these methods, the identified subgroups in this study include:

Saturated-like molecules (Sa, H/C ≥ 2.0);

Unsaturated aliphatic-like molecules (UA, 1.5 ≤ H/C < 2.0);

Highly unsaturated-like molecules (HU, $AI_{mod} \leq 0.5$ and H/C < 1.5);

Highly aromatic-like molecules (HA, $0.5 < AI_{mod} \leq 0.66$);

Polycyclic aromatic-like molecules (PA, $AI_{mod} > 0.66$).

The aromaticity equivalent (X_C), a modified index for aromatic compounds, was calculated as follows:

$$X_C = [3 \times (DBE - (p \times o + p \times s)) - 2] / [DBE - (p \times o + p \times s)] \quad (S5)$$

Here, DBE represents the double bond equivalence. p and q are the fractions of oxygen and sulfur atoms, respectively, that contribute to the π-bond structure of the molecule. In this study, $p = q = 1$ was applied for compounds detected in ESI+ and $p = q = 0.5$ was applied for compounds detected in ESI– (Wang et al., 2021a). The thresholds of $X_C \geq 2.50$ and $X_C \geq 2.71$ were used to identify monoaromatic and polyaromatic compounds, respectively (Yassine et al., 2014).

Many previous studies on organic aerosol molecular composition have utilized the peak intensities of species to highlight the relative abundance of specific compound groups (Wang et al., 2021a; Song et al., 2018; Zou et al., 2023). However, it should be

noted that different organic compounds may exhibit varying signal responses in the mass spectrometer due to differences in their ionization and transmission efficiencies (Schmidt et al., 2006; Kruve et al., 2014; Leito et al., 2008). Here, an intercomparison (mainly conducted among samples within this study) of compound relative abundance was conducted without considering the differentiation of ionization efficiency, as indicated by many previous studies (Song et al., 2018; Wang et al., 2021a; Zou et al., 2023). Furthermore, the peak intensity-weighted average molecular mass (MM), elemental ratios, DBE, X_C, AI_{mod}, and OS_C for the molecular formula $C_cH_hO_oN_n$ were calculated using the following equations:

$$MM_w = \sum (MM_i \times A_i) \,/\, \sum A_i \quad \text{(S6)}$$

$$O/C_w = \sum (O/C_i \times A_i) \,/\, \sum A_i \quad \text{(S7)}$$

$$H/C_w = \sum (H/C_i \times A_i) \,/\, \sum A_i \quad \text{(S8)}$$

$$N/C_w = \sum (N/C_i \times A_i) \,/\, \sum A_i \quad \text{(S9)}$$

$$O/N_w = \sum (O/N_i \times A_i) \,/\, \sum A_i \quad \text{(S10)}$$

$$DBE_w = \sum (DBE_i \times A_i) \,/\, \sum A_i \quad \text{(S11)}$$

$$X_{Cw} = \sum (X_{Ci} \times A_i) \,/\, \sum A_i \quad \text{(S12)}$$

$$AI_{modw} = \sum (AI_{modi} \times A_i) \,/\, \sum A_i \quad \text{(S13)}$$

$$OS_{Cw} = \sum (OS_{Ci} \times A_i) \,/\, \sum A_i \quad \text{(S14)}$$

Here, A_i represents the peak signal intensity for each individual compound *i*.

Sect. S3. The improved classification method for identifying precursors of NOCs

Identifying the precursors of aerosol NOCs is challenging due to their complex sources and variable atmospheric processes. Based on established atmospheric reactions, recent studies have identified the potential precursors of organic compounds in aerosols (Nie et al., 2022; Guo et al., 2022b). Building on these advancements, Jiang et al. (2023) further refined the classification for CHON− compounds in the ambient aerosols. In this study, we improved this identification process to classify Re-NOC precursors. Specifically, the classification of CHON+ and CHON− compounds was refined into the following categories: aliphatic-, heterocyclic-, and aromatic-derived Re-NOCs, as well as isoprene-, monoterpene-, aliphatic-, and aromatic-derived Ox-NOCs. Details of the specific classification process are illustrated in **Figure S2**. In particular, the isoprene-CHON and monoterpene-CHON lists, obtained from previous field observation and laboratory experiments (Ng et al., 2008; Xu et al., 2021b; Zhao et al., 2021; Tian et al., 2023; Wu et al., 2021; Shen et al., 2022; Draper et al., 2015; Pullinen et al., 2020; Guo et al., 2022a; Shen et al., 2021; Xu et al., 2021a; DeVault and Ziemann, 2021; Guo et al., 2022b), are summarized in **Table S2** and **Table S3**. If the identified molecular formulas were included in the aforementioned lists, these species were directly categorized as isoprene-derived CHON or monoterpene-derived CHON compounds (Jiang et al., 2023). For CHN+ compounds, they were classified into aliphatic, monoaromatic, and polyaromatic CHN+ compounds based on established criteria (Wang et al., 2021a; Yassine et al., 2014).

Sect. S4. Classification of possible aqueous-phase processes of NOCs based on precursor-product pairs

To identify potential aqueous-phase processes involved in aerosol NOC formation, we screened precursor-product pairs from the identified organic compounds. The identification of such pairs has been widely applied to infer the potential formation pathways of Ox-NOCs in urban snow, roadside ambient aerosols, and urban aerosols in China (Su et al., 2021; Xu et al., 2023; Jiang et al., 2023). The main reaction pathways proposed by the precursor-product pairs theory are detailed as follows.

Reactions of alcohols, diols, and hydroxyketones with N_2O_5 are suggested to contribute to the formation of organic nitrates (Kames et al., 1993), as shown in SR1:

$$R{-}OH + N_2O_5 \rightarrow R{-}ONO_2 + HNO_3 \quad \text{(SR1)}$$

To investigate the potential reaction products and precursors of CHON compounds, $R{-}OH$ and $R{-}ONO_2$ were defined as an oxidation-product pair. This pair is characterized by an elemental difference of $-H$ and $+NO_2$.

In addition, organic nitrates are likely hydrolyzed to alcohols at varying rates (Boyd et al., 2015; Darer et al., 2011), as simplified below (SR2).

$$R{-}(ONO_2)_2R + H_2O \rightarrow OH{-}R{-}ONO_2 + HNO_3 \quad \text{(SR2)}$$

Here, $R{-}(ONO_2)_2R$ and $OH{-}R{-}ONO_2$ were defined as a hydrolysis-product pair, characterized by an elemental difference of $+H$ and $-NO_2$. Furthermore, NOCs may also involve both oxidation and hydrolysis processes (Su et al., 2021; Jiang et al., 2023), referred to as ox_hy_N process. The remaining unidentified NOCs were attributed to unknown processes, denoted as the unknown_N process (**Fig. S5**).

The formation pathways of Re-NOCs (mainly CHON+ compounds in this study) can be classified into three main types, including condensation, hydrolysis, and dehydration processes (Sun et al., 2024). The condensation process (denoted as cond_N) can be divided into two types of reactions. One involves imination reactions (characterized by +NH and −O) between carbonyl compounds and NH_4^+ (or NH_3) (SR3), resulting in the formation of imines (Lv et al., 2022; Liu et al., 2023a; Wang et al., 2024; Abudumutailifu et al., 2024; Sun et al., 2024; Liu et al., 2023b).

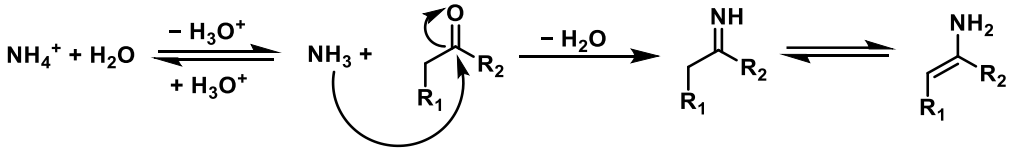

(SR3)

Another reaction involves the intramolecular N-heterocyclic pathway (characterized by +N and $-HO_2$) (SR4), which builds upon the reaction in SR3 (Laskin et al., 2010; Laskin et al., 2014; Liu et al., 2023b).

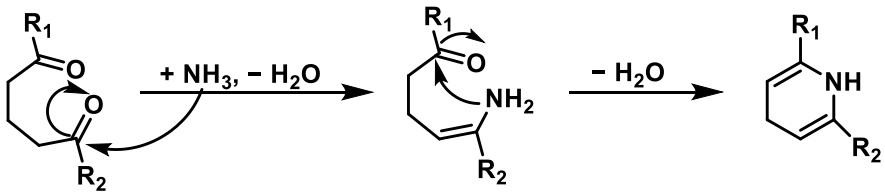

(SR4)

Recent studies suggested that dehydration processes (denoted as de_N process) may occur in aerosols and fog water (Sun et al., 2024), as well as in the photochemical transformation of organic compounds in the aqueous phase (Lian et al., 2020).

Re-NOCs can also undergo hydrolyzation processes (hy_N), which are similar to those observed in Ox-NOCs. In addition, the aqueous-phase processes of CHON+ can be associated with the aforementioned formation pathways, including cond_hy_N (involving cond_N and hy_N), cond_de_N (involving cond_N and de_N), hy_de_N

(involving hy_N and de_N), and cond_hy_de_N (involving cond_N, hy_N and de_N) (**Fig. S4)**. Another significant component of Re-NOCs is the CHN+ compounds. Since CHN+ compounds lack oxygen atoms, it is unlikely that they will be formed by hydrolysis processes. Accordingly, their potential formation mechanisms include cond_N, de_N, cond_de_N, and unknown_N pathways. The abbreviations, types, and more details for these processes were summarized in **Table S4**. The specific strategies for identifying different formation pathways of NOCs were illustrated in **Figs. S3–S5**.

Table S1. The mean values (± SD) of major parameters observed across cities and time periods.

City	HEB			BJ			HZ		
Period	All	Clean	Haze	All	Clean	Haze	All	Clean	Haze
Parameters	Mean ± SD	Mean ± SD	Mean ± SD	Mean ± SD	Mean ± SD	Mean ± SD	Mean ± SD	Mean ± SD	Mean ± SD
T (°C)	−17.3 ± 5.2	−17.0 ± 6.7	−17.6 ± 1.4	−1.6 ± 2.1	−0.9 ± 2.1	−2.9 ± 1.5	6.6 ± 2.4	5.1 ± 1.6	8.1 ± 2.1
RH (%)	66.2 ± 5.9	63.8 ± 4.2	69.4 ± 6.4	48.5 ± 20.8	35.2 ± 6.5	75.2 ± 12.0	73.8 ± 16.9	75.7 ± 17.1	72.0 ± 16.4
Wind speed (m s^{-1})	2.6 ± 0.8	3.1 ± 0.6	1.9 ± 0.6	3.2 ± 1.9	3.9 ± 1.9	1.7 ± 0.5	2.9 ± 1.1	3.3 ± 1.2	2.6 ± 0.8
$PM_{2.5}$ (μg m^{-3})	90.6 ± 62.4	45.3 ± 16.8	154.0 ± 45.3	52.7 ± 51.4	19.9 ± 11.0	118.3 ± 35.2	69.1 ± 26.9	47.4 ± 16.7	90.9 ± 14.9
O_3 (μg m^{-3})	37.8 ± 10.0	43.9 ± 7.6	29.4 ± 6.1	31.2 ± 17.5	41.0 ± 12.5	11.6 ± 5.7	26.4 ± 17.1	23.7 ± 14.3	29.1 ± 19.1
NO_2 (μg m^{-3})	52.6 ± 19.6	39.1 ± 7.7	71.3 ± 15.4	46.5 ± 22.6	33.4 ± 15.0	72.5 ± 7.8	61.6 ± 15.2	54.9 ± 14.5	68.3 ± 12.7
NO_2 + O_3 (μg m^{-3})	90.4 ± 11.7	83.0 ± 4.8	100.7 ± 10.8	77.6 ± 7.3	74.4 ± 5.9	84.0 ± 5.6	88.0 ± 17.6	78.5 ± 11.5	97.4 ± 17.5
•OH (×10^5 molecule cm^{-3})	8.1 ± 3.2	9.5 ± 3.0	6.3 ± 2.4	9.8 ± 4.7	12.8 ± 2.1	3.7 ± 1.3	4.9 ± 3.1	4.5 ± 3.4	5.2 ± 2.8
SO_2 (μg m^{-3})	56.2 ± 18.0	44.4 ± 9.5	72.7 ± 13.7	7.0 ± 3.2	6.1 ± 2.9	8.7 ± 3.1	13.1 ± 3.4	11.6 ± 2.5	14.6 ± 3.5
CO (mg m^{-3})	1.2 ± 0.5	0.8 ± 0.1	1.8 ± 0.4	1.1 ± 0.8	0.7 ± 0.3	2.1 ± 0.5	1.2 ± 0.2	1.1 ± 0.2	1.3 ± 0.1
ALW[a] (μg m^{-3})	31.5 ± 23.6	17.3 ± 12.6	51.4 ± 20.9	48.9 ± 109.6	4.8 ± 2.6	136.9 ± 156.3	64.6 ± 66.1	52.1 ± 42.8	77.2 ± 81.2
pH	4.3 ± 1.0	4.0 ± 1.2	4.9 ± 0.3	6.3 ± 1.7	7.4 ± 0.8	4.1 ± 0.6	3.4 ± 0.6	3.5 ± 0.3	3.2 ± 0.7
PBLH[b] (m)	339.0 ± 183.3	457.3 ± 150.4	173.4 ± 44.2	407.9 ± 313.3	501 ± 335.9	221.6 ± 129.1	414.1 ± 239.0	445 ± 226.5	383.2 ± 247.0
VC[c] (m^2 s^{-1})	974.8 ± 673.2	1415.1 ± 530.5	358.5 ± 206.0	1877.4 ± 2608.4	2592.4 ± 2931.7	447.4 ± 393.9	1431.2 ± 1200.3	1692.5 ± 1318.0	1169.8 ± 1003.8
UV (W m^{-2})	71.1 ± 6.1	70.3 ± 6.2	72.3 ± 5.7	112.9 ± 8.7	112.2 ± 10.3	114.3 ± 3.6	128.1 ± 56.6	134.2 ± 62.3	122 ± 49.4
Cl^- (μg m^{-3})	5.9 ± 4.9	3.2 ± 2.3	9.7 ± 5.0	2.7 ± 1.9	1.7 ± 1.0	4.6 ± 1.7	2.1 ± 1.1	1.6 ± 1.1	2.6 ± 0.8
Nss-Cl^- (μg m^{-3})	5.2 ± 4.2	2.8 ± 2.1	8.5 ± 4.3	2.0 ± 1.8	1.1 ± 0.8	3.8 ±1.9	1.6 ±1.0	1.1 ±1.0	2.0 ±0.8
NO_3^- (μg m^{-3})	9.2 ± 6.4	7.7 ± 7.2	11.3 ± 4.2	10.8 ± 14.6	2.6 ± 1.8	27.1 ± 15.3	18.9 ± 7.7	13.0 ± 5.2	24.8 ± 4.8
SO_4^{2-} (μg m^{-3})	11.4 ± 7.0	7.3 ± 3.5	17.3 ± 6.6	7.4 ± 8.1	2.7 ± 1.0	16.9 ± 7.7	9.9 ± 3.5	8.0 ± 3.1	11.8 ± 2.9
NO_3^-/SO_4^{2-}	0.8 ± 0.4	0.9 ± 0.5	0.7 ± 0.2	1.1 ± 0.5	1.0 ± 0.4	1.5 ± 0.4	2.0 ± 0.7	1.8 ± 0.9	2.1 ± 0.3
NH_4^+/NO_3^-	1.0 ± 0.2	0.9 ± 0.3	1.1 ± 0.3	0.7 ± 0.1	0.7 ± 0.1	0.6 ± 0.1	0.5 ± 0.1	0.5 ± 0.1	0.4 ± 0.1
K^+ (μg m^{-3})	1.9 ± 1.3	1.1 ± 0.7	3.0 ± 1.3	0.6 ± 0.5	0.4 ± 0.3	1.0 ± 0.5	0.8 ± 0.3	0.6 ± 0.2	0.9 ± 0.2
Nss-K^+ (μg m^{-3})	1.9 ± 1.3	1.1 ± 0.6	3.0 ± 1.3	0.6 ± 0.5	0.4 ± 0.3	1.0 ± 0.5	0.8 ± 0.3	0.6 ± 0.2	0.9 ± 0.2
Na^+ (μg m^{-3})	0.4 ± 0.4	0.2 ± 0.1	0.7 ± 0.4	0.4 ± 0.2	0.3 ± 0.1	0.5 ± 0.2	0.3 ± 0.1	0.3 ± 0.1	0.3 ± 0.1
Ca^{2+} (μg m^{-3})	0.9 ± 0.4	0.7 ± 0.3	1.2 ± 0.3	2.3 ± 0.7	2.7 ± 0.2	1.6 ± 0.8	2.2 ± 1.5	1.9 ± 1.3	2.4 ± 1.7

NH_4^+ (μg m^{-3})	8.2 ± 5.5	5.3 ± 3.4	12.4 ± 5.1	6.6 ± 9.1	1.7 ± 1.1	16.3 ± 10.2	8.3 ± 2.9	6.2 ± 1.5	10.4 ± 2.4
HCOOH (μg m^{-3})	0.2 ± 0.2	0.10 ± 0.07	0.43 ± 0.25	0.07 ± 0.09	0.03 ± 0.04	0.14 ± 0.13	0.03 ± 0.02	0.02 ± 0.01	0.04 ± 0.02
CH_3COOH (μg m^{-3})	0.3 ± 0.2	0.18 ± 0.11	0.43 ± 0.24	0.06 ± 0.07	0.04 ± 0.04	0.11 ± 0.08	0.06 ± 0.04	0.07 ± 0.04	0.04 ± 0.02
$C_2H_2O_4$ (μg m^{-3})	0.4 ± 0.2	0.25 ± 0.19	0.48 ± 0.10	0.21 ± 0.18	0.11 ± 0.05	0.40 ± 0.18	0.2 ± 0.22	0.08 ± 0.1	0.2 ± 0.3
$C_4H_6O_4$ (μg m^{-3})	0.3 ± 0.3	0.3 ± 0.3	0.2 ± 0.2	0.03 ± 0.04	0.01 ± 0.01	0.06 ± 0.05	0.007 ± 0.004	0.006 ± 0.005	0.008 ± 0.002
$C_5H_8O_4$ (μg m^{-3})	0.1 ± 0.04	0.02 ± 0.01	0.07 ± 0.04	0.02 ± 0.01	0.01 ± 0.002	0.04 ± 0.005	0.007 ± 0.008	0 .005± 0.003	0.009 ± 0.010
CH_4O_3S (μg m^{-3})	0.03 ± 0.02	0.02 ± 0.02	0.04 ± 0.01	0.06 ± 0.05	0.01 ± 0.001	0.07 ± 0.05	0.051 ± 0.027	0.03 ± 0.02	0.07 ± 0.02

[a]Aerosol liquid water.

[b]Planetary boundary layer height.

[c]Ventilation coefficient.

Table S2. List of molecular formulas for potential isoprene-derived CHON compounds.

Formula[a]	C	H	N	O
$C_4H_7N_1O_5$	4	7	1	5
$C_4H_7N_1O_6$	4	7	1	6
$C_4H_7N_1O_7$	4	7	1	7
$C_4H_9N_1O_7$	4	9	1	7
$C_4H_7N_1O_8$	4	7	1	8
$C_4H_7N_1O_9$	4	7	1	9
$C_4H_6N_2O_6$	4	6	2	6
$C_4H_6N_2O_7$	4	6	2	7
$C_4H_8N_2O_7$	4	8	2	7
$C_4H_6N_2O_8$	4	6	2	8
$C_4H_8N_2O_8$	4	8	2	8
$C_4H_7N_2O_9$	4	7	2	9
$C_4H_8N_2O_9$	4	8	2	9
$C_4H_8N_2O_{10}$	4	8	2	10
$C_4H_7N_3O_9$	4	7	3	9
$C_4H_7N_3O_{10}$	4	7	3	10
$C_4H_7N_3O_{11}$	4	7	3	11
$C_5H_7N_1O_4$	5	7	1	4
$C_5H_9N_1O_4$	5	9	1	4
$C_5H_7N_1O_5$	5	7	1	5
$C_5H_9N_1O_5$	5	9	1	5
$C_5H_7N_1O_6$	5	7	1	6
$C_5H_9N_1O_6$	5	9	1	6
$C_5H_{11}N_1O_6$	5	11	1	6
$C_5H_7N_1O_7$	5	7	1	7
$C_5H_9N_1O_7$	5	9	1	7
$C_5H_{11}N_1O_7$	5	11	1	7
$C_5H_7N_1O_8$	5	7	1	8
$C_5H_8N_1O_8$	5	8	1	8
$C_5H_9N_1O_8$	5	9	1	8
$C_5H_{11}N_1O_8$	5	11	1	8
$C_5H_7N_1O_9$	5	7	1	9
$C_5H_8N_1O_9$	5	8	1	9
$C_5H_9N_1O_9$	5	9	1	9
$C_5H_{11}N_1O_9$	5	11	1	9
$C_5H_{13}N_1O_9$	5	13	1	9
$C_5H_8N_1O_{10}$	5	8	1	10
$C_5H_9N_1O_{10}$	5	9	1	10
$C_5H_{11}N_1O_{10}$	5	11	1	10
$C_5H_{10}N_1O_{11}$	5	10	1	11
$C_5H_{10}N_2O_6$	5	10	2	6
$C_5H_8N_2O_7$	5	8	2	7

$C_5H_{10}N_2O_7$	5	10	2	7
$C_5H_6N_2O_8$	5	6	2	8
$C_5H_8N_2O_8$	5	8	2	8
$C_5H_{10}N_2O_8$	5	10	2	8
$C_5H_8N_2O_9$	5	8	2	9
$C_5H_9N_2O_9$	5	9	2	9
$C_5H_{10}N_2O_9$	5	10	2	9
$C_5H_{12}N_2O_9$	5	12	2	9
$C_5H_8N_2O_{10}$	5	8	2	10
$C_5H_9N_2O_{10}$	5	9	2	10
$C_5H_{10}N_2O_{10}$	5	10	2	10
$C_5H_{12}N_2O_{10}$	5	12	2	10
$C_5H_8N_2O_{11}$	5	8	2	11
$C_5H_{10}N_2O_{11}$	5	10	2	11
$C_5H_{12}N_2O_{11}$	5	12	2	11
$C_5H_9N_3O_9$	5	9	3	9
$C_5H_{11}N_3O_9$	5	11	3	9
$C_5H_9N_3O_{10}$	5	9	3	10
$C_5H_{11}N_3O_{10}$	5	11	3	10
$C_5H_9N_3O_{11}$	5	9	3	11
$C_5H_{11}N_3O_{11}$	5	11	3	11
$C_5H_9N_3O_{12}$	5	9	3	12
$C_5H_9N_3O_{13}$	5	9	3	13
$C_5H_{11}N_3O_{13}$	5	11	3	13
$C_5H_9N_4O_{12}$	5	9	4	12
$C_5H_{10}N_4O_{12}$	5	10	4	12
$C_5H_{10}N_4O_{13}$	5	10	4	13
$C_{10}H_{15}N_1O_{10}$	10	15	1	10
$C_{10}H_{16}N_2O_8$	10	16	2	8
$C_{10}H_{16}N_2O_9$	10	16	2	9
$C_{10}H_{16}N_2O_{10}$	10	16	2	10
$C_{10}H_{16}N_2O_{11}$	10	16	2	11
$C_{10}H_{18}N_2O_{11}$	10	18	2	11
$C_{10}H_{16}N_2O_{12}$	10	16	2	12
$C_{10}H_{16}N_2O_{13}$	10	16	2	13
$C_{10}H_{16}N_2O_{14}$	10	16	2	14
$C_{10}H_{16}N_2O_{15}$	10	16	2	15
$C_{10}H_{16}N_2O_{17}$	10	16	2	17
$C_{10}H_{17}N_3O_{12}$	10	17	3	12
$C_{10}H_{13}N_3O_{13}$	10	13	3	13
$C_{10}H_{17}N_3O_{13}$	10	17	3	13
$C_{10}H_{15}N_3O_{14}$	10	15	3	14
$C_{10}H_{17}N_3O_{14}$	10	17	3	14

$C_{10}H_{17}N_3O_{15}$	10	17	3	15
$C_{10}H_{17}N_3O_{16}$	10	17	3	16
$C_{10}H_{17}N_3O_{17}$	10	17	3	17
$C_{10}H_{17}N_3O_{18}$	10	17	3	18
$C_{10}H_{18}N_4O_{16}$	10	18	4	16
$C_{10}H_{18}N_4O_{17}$	10	18	4	17
$C_{10}H_{17}N_5O_{18}$	10	17	5	18
$C_{15}H_{24}N_4O_{18}$	15	24	4	18
$C_{15}H_{24}N_4O_{21}$	15	24	4	21
$C_{15}H_{24}N_4O_{22}$	15	24	4	22
$C_{15}H_{25}N_5O_{21}$	15	25	5	21

[a]The molecular formulas were summarized from previous studies (Ng et al., 2008; Guo et al., 2022b; Xu et al., 2021b; Zhao et al., 2021; Tian et al., 2023; Wu et al., 2021).

Table S3. List of molecular formulas for potential monoterpene-derived CHON compounds.

Formula[a]	C	H	N	O
$C_6H_7N_1O_6$	6	7	1	6
$C_6H_7N_1O_7$	6	7	1	7
$C_6H_7N_1O_8$	6	7	1	8
$C_6H_9N_1O_9$	6	9	1	9
$C_6H_7N_1O_{10}$	6	7	1	10
$C_6H_7N_1O_{11}$	6	7	1	11
$C_6H_6N_2O_9$	6	6	2	9
$C_6H_{10}N_2O_{10}$	6	10	2	10
$C_7H_9N_1O_5$	7	9	1	5
$C_7H_{11}N_1O_5$	7	11	1	5
$C_7H_9N_1O_6$	7	9	1	6
$C_7H_{11}N_1O_6$	7	11	1	6
$C_7H_7N_1O_7$	7	7	1	7
$C_7H_9N_1O_7$	7	9	1	7
$C_7H_{11}N_1O_7$	7	11	1	7
$C_7H_7N_1O_8$	7	7	1	8
$C_7H_8N_1O_8$	7	8	1	8
$C_7H_9N_1O_8$	7	9	1	8
$C_7H_{10}N_1O_8$	7	10	1	8
$C_7H_{11}N_1O_8$	7	11	1	8
$C_7H_9N_1O_9$	7	9	1	9
$C_7H_{10}N_1O_9$	7	10	1	9
$C_7H_{11}N_1O_9$	7	11	1	9
$C_7H_9N_1O_{10}$	7	9	1	10
$C_7H_{10}N_1O_{10}$	7	10	1	10
$C_7H_{11}N_1O_{10}$	7	11	1	10
$C_7H_9N_1O_{11}$	7	9	1	11
$C_7H_{10}N_1O_{11}$	7	10	1	11
$C_7H_{11}N_1O_{11}$	7	11	1	11
$C_7H_9N_1O_{12}$	7	9	1	12
$C_7H_{10}N_1O_{12}$	7	10	1	12
$C_7H_{11}N_1O_{12}$	7	11	1	12
$C_7H_{11}N_1O_{15}$	7	11	1	15
$C_7H_8N_2O_8$	7	8	2	8
$C_7H_8N_2O_{10}$	7	8	2	10
$C_7H_8N_2O_{11}$	7	8	2	11
$C_7H_8N_2O_{12}$	7	8	2	12
$C_7H_8N_2O_{13}$	7	8	2	13
$C_7H_8N_2O_{14}$	7	8	2	14
$C_7H_{10}N_2O_{14}$	7	10	2	14
$C_8H_{13}N_1O_5$	8	13	1	5

$C_8H_{17}N_1O_5$	8	17	1	5
$C_8H_{11}N_1O_6$	8	11	1	6
$C_8H_{11}N_1O_7$	8	11	1	7
$C_8H_{12}N_1O_7$	8	12	1	7
$C_8H_{11}N_1O_8$	8	11	1	8
$C_8H_{12}N_1O_8$	8	12	1	8
$C_8H_{13}N_1O_8$	8	13	1	8
$C_8H_{15}N_1O_8$	8	15	1	8
$C_8H_{11}N_1O_9$	8	11	1	9
$C_8H_{12}N_1O_9$	8	12	1	9
$C_8H_{13}N_1O_9$	8	13	1	9
$C_8H_{11}N_1O_{10}$	8	11	1	10
$C_8H_{12}N_1O_{10}$	8	12	1	10
$C_8H_{13}N_1O_{10}$	8	13	1	10
$C_8H_{11}N_1O_{11}$	8	11	1	11
$C_8H_{12}N_1O_{11}$	8	12	1	11
$C_8H_{13}N_1O_{11}$	8	13	1	11
$C_8H_{11}N_1O_{12}$	8	11	1	12
$C_8H_{12}N_1O_{12}$	8	12	1	12
$C_8H_{13}N_1O_{12}$	8	13	1	12
$C_8H_{11}N_1O_{13}$	8	11	1	13
$C_8H_{10}N_2O_8$	8	10	2	8
$C_8H_{10}N_2O_{14}$	8	10	2	14
$C_9H_{11}N_1O_2$	9	11	1	2
$C_9H_{13}N_1O_2$	9	13	1	2
$C_9H_{17}N_1O_3$	9	17	1	3
$C_9H_{13}N_1O_4$	9	13	1	4
$C_9H_{14}N_1O_4$	9	14	1	4
$C_9H_{15}N_1O_4$	9	15	1	4
$C_9H_{11}N_1O_5$	9	11	1	5
$C_9H_{13}N_1O_5$	9	13	1	5
$C_9H_{12}N_1O_6$	9	12	1	6
$C_9H_{13}N_1O_6$	9	13	1	6
$C_9H_{16}N_1O_6$	9	16	1	6
$C_9H_{13}N_1O_7$	9	13	1	7
$C_9H_{14}N_1O_7$	9	14	1	7
$C_9H_{15}N_1O_7$	9	15	1	7
$C_9H_{13}N_1O_8$	9	13	1	8
$C_9H_{14}N_1O_8$	9	14	1	8
$C_9H_{15}N_1O_8$	9	15	1	8
$C_9H_{16}N_1O_8$	9	16	1	8
$C_9H_{13}N_1O_9$	9	13	1	9
$C_9H_{14}N_1O_9$	9	14	1	9
$C_9H_{15}N_1O_9$	9	15	1	9

$C_9H_{13}N_1O_{10}$	9	13	1	10
$C_9H_{14}N_1O_{10}$	9	14	1	10
$C_9H_{15}N_1O_{10}$	9	15	1	10
$C_9H_{13}N_1O_{11}$	9	13	1	11
$C_9H_{14}N_1O_{11}$	9	14	1	11
$C_9H_{15}N_1O_{11}$	9	15	1	11
$C_9H_{13}N_1O_{12}$	9	13	1	12
$C_9H_{14}N_1O_{12}$	9	14	1	12
$C_9H_{15}N_1O_{12}$	9	15	1	12
$C_9H_{13}N_1O_{13}$	9	13	1	13
$C_9H_{14}N_1O_{13}$	9	14	1	13
$C_9H_{15}N_1O_{13}$	9	15	1	13
$C_9H_{13}N_1O_{14}$	9	13	1	14
$C_9H_{14}N_1O_{14}$	9	14	1	14
$C_9H_{15}N_1O_{14}$	9	15	1	14
$C_9H_{13}N_2O_7$	9	13	2	7
$C_9H_{14}N_2O_8$	9	14	2	8
$C_9H_{10}N_2O_9$	9	10	2	9
$C_9H_{11}N_2O_9$	9	11	2	9
$C_9H_{12}N_2O_9$	9	12	2	9
$C_9H_{10}N_2O_{10}$	9	10	2	10
$C_9H_{11}N_2O_{10}$	9	11	2	10
$C_9H_{12}N_2O_{10}$	9	12	2	10
$C_9H_{10}N_2O_{11}$	9	10	2	11
$C_9H_{11}N_2O_{11}$	9	11	2	11
$C_9H_{12}N_2O_{11}$	9	12	2	11
$C_9H_{10}N_2O_{12}$	9	10	2	12
$C_9H_{11}N_2O_{12}$	9	11	2	12
$C_9H_{12}N_2O_{12}$	9	12	2	12
$C_9H_{14}N_2O_{12}$	9	14	2	12
$C_{10}H_{15}N_1O_3$	10	15	1	3
$C_{10}H_{17}N_1O_3$	10	17	1	3
$C_{10}H_{15}N_1O_4$	10	15	1	4
$C_{10}H_{17}N_1O_4$	10	17	1	4
$C_{10}H_{19}N_1O_4$	10	19	1	4
$C_{10}H_{15}N_1O_5$	10	15	1	5
$C_{10}H_{17}N_1O_5$	10	17	1	5
$C_{10}H_{13}N_1O_6$	10	13	1	6
$C_{10}H_{15}N_1O_6$	10	15	1	6
$C_{10}H_{16}N_1O_6$	10	16	1	6
$C_{10}H_{17}N_1O_6$	10	17	1	6
$C_{10}H_{13}N_1O_7$	10	13	1	7
$C_{10}H_{15}N_1O_7$	10	15	1	7
$C_{10}H_{16}N_1O_7$	10	16	1	7

$C_{10}H_{17}N_1O_7$	10	17	1	7
$C_{10}H_{13}N_1O_8$	10	13	1	8
$C_{10}H_{15}N_1O_8$	10	15	1	8
$C_{10}H_{16}N_1O_8$	10	16	1	8
$C_{10}H_{17}N_1O_8$	10	17	1	8
$C_{10}H_{13}N_1O_9$	10	13	1	9
$C_{10}H_{15}N_1O_9$	10	15	1	9
$C_{10}H_{16}N_1O_9$	10	16	1	9
$C_{10}H_{17}N_1O_9$	10	17	1	9
$C_{10}H_{15}N_1O_{10}$	10	15	1	10
$C_{10}H_{16}N_1O_{10}$	10	16	1	10
$C_{10}H_{17}N_1O_{10}$	10	17	1	10
$C_{10}H_{15}N_1O_{11}$	10	15	1	11
$C_{10}H_{16}N_1O_{11}$	10	16	1	11
$C_{10}H_{17}N_1O_{11}$	10	17	1	11
$C_{10}H_{18}N_1O_{11}$	10	18	1	11
$C_{10}H_{15}N_1O_{12}$	10	15	1	12
$C_{10}H_{16}N_1O_{12}$	10	16	1	12
$C_{10}H_{17}N_1O_{12}$	10	17	1	12
$C_{10}H_{15}N_1O_{13}$	10	15	1	13
$C_{10}H_{16}N_1O_{13}$	10	16	1	13
$C_{10}H_{17}N_1O_{13}$	10	17	1	13
$C_{10}H_{15}N_1O_{14}$	10	15	1	14
$C_{10}H_{16}N_1O_{14}$	10	16	1	14
$C_{10}H_{17}N_1O_{14}$	10	17	1	14
$C_{10}H_{15}N_1O_{15}$	10	15	1	15
$C_{10}H_{16}N_1O_{15}$	10	16	1	15
$C_{10}H_{17}N_1O_{15}$	10	17	1	15
$C_{10}H_{12}N_2O_5$	10	12	2	5
$C_{10}H_{20}N_2O_6$	10	20	2	6
$C_{10}H_{12}N_2O_8$	10	12	2	8
$C_{10}H_{14}N_2O_8$	10	14	2	8
$C_{10}H_{15}N_2O_8$	10	15	2	8
$C_{10}H_{16}N_2O_8$	10	16	2	8
$C_{10}H_{18}N_2O_8$	10	18	2	8
$C_{10}H_{12}N_2O_9$	10	12	2	9
$C_{10}H_{14}N_2O_9$	10	14	2	9
$C_{10}H_{15}N_2O_9$	10	15	2	9
$C_{10}H_{16}N_2O_9$	10	16	2	9
$C_{10}H_{18}N_2O_9$	10	18	2	9
$C_{10}H_{12}N_2O_{10}$	10	12	2	10
$C_{10}H_{14}N_2O_{10}$	10	14	2	10
$C_{10}H_{15}N_2O_{10}$	10	15	2	10
$C_{10}H_{16}N_2O_{10}$	10	16	2	10

$C_{10}H_{14}N_2O_{11}$	10	14	2	11
$C_{10}H_{15}N_2O_{11}$	10	15	2	11
$C_{10}H_{16}N_2O_{11}$	10	16	2	11
$C_{10}H_{14}N_2O_{12}$	10	14	2	12
$C_{10}H_{15}N_2O_{12}$	10	15	2	12
$C_{10}H_{16}N_2O_{12}$	10	16	2	12
$C_{10}H_{17}N_2O_{12}$	10	17	2	12
$C_{10}H_{14}N_2O_{13}$	10	14	2	13
$C_{10}H_{15}N_2O_{13}$	10	15	2	13
$C_{10}H_{16}N_2O_{13}$	10	16	2	13
$C_{10}H_{18}N_2O_{13}$	10	18	2	13
$C_{10}H_{14}N_2O_{14}$	10	14	2	14
$C_{10}H_{15}N_2O_{14}$	10	15	2	14
$C_{10}H_{16}N_2O_{14}$	10	16	2	14
$C_{10}H_{18}N_2O_{14}$	10	18	2	14
$C_{10}H_{14}N_2O_{15}$	10	14	2	15
$C_{10}H_{15}N_2O_{15}$	10	15	2	15
$C_{10}H_{16}N_2O_{15}$	10	16	2	15
$C_{10}H_{14}N_2O_{16}$	10	14	2	16
$C_{10}H_{15}N_2O_{16}$	10	15	2	16
$C_{10}H_{16}N_2O_{16}$	10	16	2	16
$C_{10}H_{15}N_3O_{11}$	10	15	3	11
$C_{10}H_{17}N_3O_{12}$	10	17	3	12
$C_{10}H_{15}N_3O_{13}$	10	15	3	13
$C_{10}H_{17}N_3O_{13}$	10	17	3	13
$C_{10}H_{15}N_3O_{14}$	10	15	3	14
$C_{10}H_{17}N_3O_{14}$	10	17	3	14
$C_{10}H_{15}N_3O_{15}$	10	15	3	15
$C_{10}H_{17}N_3O_{15}$	10	17	3	15
$C_{10}H_{17}N_3O_{16}$	10	17	3	16
$C_{11}H_{23}N_1O_3$	11	23	1	3
$C_{11}H_{17}N_1O_5$	11	17	1	5
$C_{11}H_{20}N_2O_5$	11	20	2	5
$C_{11}H_{18}N_2O_{10}$	11	18	2	10
$C_{12}H_{23}N_1O_3$	12	23	1	3
$C_{13}H_{25}N_1O_2$	13	25	1	2
$C_{13}H_{26}N_1O_{12}$	13	26	1	12
$C_{14}H_{26}N_1O_{10}$	14	26	1	10
$C_{14}H_{24}N_2O_5$	14	24	2	5
$C_{15}H_{30}N_1O_{14}$	15	30	1	14
$C_{16}H_{35}N_1O_3$	16	35	1	3
$C_{16}H_{32}N_1O_{13}$	16	32	1	13
$C_{16}H_{32}N_1O_{14}$	16	32	1	14
$C_{16}H_{32}N_1O_{15}$	16	32	1	15

$C_{17}H_{22}N_1O_6$	17	22	1	6
$C_{17}H_{28}N_1O_9$	17	28	1	9
$C_{17}H_{27}N_1O_{12}$	17	27	1	12
$C_{17}H_{32}N_1O_{13}$	17	32	1	13
$C_{17}H_{34}N_1O_{13}$	17	34	1	13
$C_{17}H_{34}N_1O_{14}$	17	34	1	14
$C_{17}H_{27}N_1O_{15}$	17	27	1	15
$C_{17}H_{34}N_1O_{15}$	17	34	1	15
$C_{17}H_{28}N_2O_9$	17	28	2	9
$C_{17}H_{26}N_2O_{12}$	17	26	2	12
$C_{17}H_{26}N_2O_{13}$	17	26	2	13
$C_{17}H_{28}N_2O_{13}$	17	28	2	13
$C_{17}H_{26}N_2O_{14}$	17	26	2	14
$C_{17}H_{26}N_2O_{15}$	17	26	2	15
$C_{17}H_{26}N_2O_{16}$	17	26	2	16
$C_{17}H_{26}N_2O_{17}$	17	26	2	17
$C_{17}H_{26}N_2O_{18}$	17	26	2	18
$C_{18}H_{27}N_1O_5$	18	27	1	5
$C_{18}H_{31}N_1O_7$	18	31	1	7
$C_{18}H_{31}N_1O_8$	18	31	1	8
$C_{18}H_{27}N_1O_{10}$	18	27	1	10
$C_{18}H_{28}N_1O_{13}$	18	28	1	13
$C_{18}H_{32}N_1O_{14}$	18	32	1	14
$C_{18}H_{34}N_1O_{14}$	18	34	1	14
$C_{18}H_{36}N_1O_{14}$	18	36	1	14
$C_{18}H_{29}N_1O_{15}$	18	29	1	15
$C_{18}H_{34}N_1O_{15}$	18	34	1	15
$C_{18}H_{36}N_1O_{15}$	18	36	1	15
$C_{18}H_{35}N_1O$	18	35	1	1
$C_{18}H_{34}N_2O_5$	18	34	2	5
$C_{18}H_{30}N_2O_7$	18	30	2	7
$C_{18}H_{28}N_2O_{11}$	18	28	2	11
$C_{18}H_{28}N_2O_{12}$	18	28	2	12
$C_{18}H_{29}N_3O_{13}$	18	29	3	13
$C_{18}H_{29}N_3O_{14}$	18	29	3	14
$C_{19}H_{41}N_1O_2$	19	41	1	2
$C_{19}H_{38}N_1O_3$	19	38	1	3
$C_{19}H_{29}N_1O_4$	19	29	1	4
$C_{19}H_{29}N_1O_5$	19	29	1	5
$C_{19}H_{33}N_1O_5$	19	33	1	5
$C_{19}H_{29}N_1O_6$	19	29	1	6
$C_{19}H_{33}N_1O_6$	19	33	1	6
$C_{19}H_{31}N_1O_7$	19	31	1	7
$C_{19}H_{33}N_1O_7$	19	33	1	7

$C_{19}H_{35}N_1O_7$	19	35	1	7
$C_{19}H_{33}N_1O_8$	19	33	1	8
$C_{19}H_{35}N_1O_8$	19	35	1	8
$C_{19}H_{29}N_1O_{10}$	19	29	1	10
$C_{19}H_{31}N_1O_{10}$	19	31	1	10
$C_{19}H_{29}N_1O_{11}$	19	29	1	11
$C_{19}H_{31}N_1O_{11}$	19	31	1	11
$C_{19}H_{29}N_1O_{12}$	19	29	1	12
$C_{19}H_{31}N_1O_{12}$	19	31	1	12
$C_{19}H_{29}N_1O_{13}$	19	29	1	13
$C_{19}H_{31}N_1O_{13}$	19	31	1	13
$C_{19}H_{31}N_1O_{14}$	19	31	1	14
$C_{19}H_{38}N_1O_{14}$	19	38	1	14
$C_{19}H_{31}N_1O_{15}$	19	31	1	15
$C_{19}H_{38}N_1O_{15}$	19	38	1	15
$C_{19}H_{38}N_1O_{16}$	19	38	1	16
$C_{19}H_{30}N_1O_{17}$	19	30	1	17
$C_{19}H_{36}N_1O_{17}$	19	36	1	17
$C_{19}H_{24}N_2O_2$	19	24	2	2
$C_{19}H_{34}N_2O_8$	19	34	2	8
$C_{19}H_{30}N_2O_{10}$	19	30	2	10
$C_{19}H_{30}N_2O_{11}$	19	30	2	11
$C_{19}H_{30}N_2O_{12}$	19	30	2	12
$C_{19}H_{30}N_2O_{13}$	19	30	2	13
$C_{19}H_{30}N_2O_{14}$	19	30	2	14
$C_{19}H_{32}N_2O_{14}$	19	32	2	14
$C_{19}H_{30}N_2O_{15}$	19	30	2	15
$C_{19}H_{30}N_2O_{16}$	19	30	2	16
$C_{19}H_{30}N_2O_{17}$	19	30	2	17
$C_{19}H_{30}N_2O_{18}$	19	30	2	18
$C_{19}H_{30}N_2O_{19}$	19	30	2	19
$C_{19}H_{31}N_3O_{15}$	19	31	3	15
$C_{19}H_{31}N_3O_{16}$	19	31	3	16
$C_{19}H_{31}N_3O_{17}$	19	31	3	17
$C_{19}H_{31}N_3O_{18}$	19	31	3	18
$C_{19}H_{31}N_3O_{19}$	19	31	3	19
$C_{19}H_{30}N_4O_{13}$	19	30	4	13
$C_{19}H_{30}N_4O_{15}$	19	30	4	15
$C_{19}H_{31}N_5O_{17}$	19	31	5	17
$C_{19}H_{31}N_5O_{18}$	19	31	5	18
$C_{19}H_{31}N_5O_{19}$	19	31	5	19
$C_{20}H_{31}N_1O_4$	20	31	1	4
$C_{20}H_{31}N_1O_5$	20	31	1	5
$C_{20}H_{35}N_1O_5$	20	35	1	5

$C_{20}H_{31}N_1O_6$	20	31	1	6
$C_{20}H_{33}N_1O_6$	20	33	1	6
$C_{20}H_{35}N_1O_6$	20	35	1	6
$C_{20}H_{31}N_1O_7$	20	31	1	7
$C_{20}H_{33}N_1O_7$	20	33	1	7
$C_{20}H_{35}N_1O_7$	20	35	1	7
$C_{20}H_{37}N_1O_7$	20	37	1	7
$C_{20}H_{31}N_1O_8$	20	31	1	8
$C_{20}H_{33}N_1O_8$	20	33	1	8
$C_{20}H_{31}N_1O_9$	20	31	1	9
$C_{20}H_{33}N_1O_9$	20	33	1	9
$C_{20}H_{39}N_1O_9$	20	39	1	9
$C_{20}H_{31}N_1O_{10}$	20	31	1	10
$C_{20}H_{31}N_1O_{11}$	20	31	1	11
$C_{20}H_{31}N_1O_{12}$	20	31	1	12
$C_{20}H_{33}N_1O_{12}$	20	33	1	12
$C_{20}H_{31}N_1O_{13}$	20	31	1	13
$C_{20}H_{40}N_1O_{14}$	20	40	1	14
$C_{20}H_{31}N_1O_{15}$	20	31	1	15
$C_{20}H_{33}N_1O_{15}$	20	33	1	15
$C_{20}H_{38}N_1O_{15}$	20	38	1	15
$C_{20}H_{40}N_1O_{15}$	20	40	1	15
$C_{20}H_{33}N_1O_{16}$	20	33	1	16
$C_{20}H_{38}N_1O_{16}$	20	38	1	16
$C_{20}H_{40}N_1O_{16}$	20	40	1	16
$C_{20}H_{32}N_2O_8$	20	32	2	8
$C_{20}H_{34}N_2O_8$	20	34	2	8
$C_{20}H_{30}N_2O_9$	20	30	2	9
$C_{20}H_{32}N_2O_9$	20	32	2	9
$C_{20}H_{32}N_2O_{10}$	20	32	2	10
$C_{20}H_{32}N_2O_{11}$	20	32	2	11
$C_{20}H_{34}N_2O_{11}$	20	34	2	11
$C_{20}H_{30}N_2O_{12}$	20	30	2	12
$C_{20}H_{32}N_2O_{12}$	20	32	2	12
$C_{20}H_{30}N_2O_{13}$	20	30	2	13
$C_{20}H_{31}N_2O_{13}$	20	31	2	13
$C_{20}H_{32}N_2O_{13}$	20	32	2	13
$C_{20}H_{30}N_2O_{14}$	20	30	2	14
$C_{20}H_{31}N_2O_{14}$	20	31	2	14
$C_{20}H_{32}N_2O_{14}$	20	32	2	14
$C_{20}H_{30}N_2O_{15}$	20	30	2	15
$C_{20}H_{31}N_2O_{15}$	20	31	2	15
$C_{20}H_{32}N_2O_{15}$	20	32	2	15
$C_{20}H_{30}N_2O_{16}$	20	30	2	16

$C_{20}H_{31}N_2O_{16}$	20	31	2	16
$C_{20}H_{32}N_2O_{16}$	20	32	2	16
$C_{20}H_{30}N_2O_{17}$	20	30	2	17
$C_{20}H_{32}N_2O_{17}$	20	32	2	17
$C_{20}H_{32}N_2O_{18}$	20	32	2	18
$C_{20}H_{32}N_2O_{19}$	20	32	2	19
$C_{20}H_{32}N_2O_{20}$	20	32	2	20
$C_{20}H_{31}N_3O_{12}$	20	31	3	12
$C_{20}H_{33}N_3O_{12}$	20	33	3	12
$C_{20}H_{31}N_3O_{13}$	20	31	3	13
$C_{20}H_{33}N_3O_{13}$	20	33	3	13
$C_{20}H_{31}N_3O_{14}$	20	31	3	14
$C_{20}H_{33}N_3O_{14}$	20	33	3	14
$C_{20}H_{31}N_3O_{15}$	20	31	3	15
$C_{20}H_{33}N_3O_{15}$	20	33	3	15
$C_{20}H_{31}N_3O_{16}$	20	31	3	16
$C_{20}H_{32}N_3O_{16}$	20	32	3	16
$C_{20}H_{33}N_3O_{16}$	20	33	3	16
$C_{20}H_{31}N_3O_{17}$	20	31	3	17
$C_{20}H_{32}N_3O_{17}$	20	32	3	17
$C_{20}H_{33}N_3O_{17}$	20	33	3	17
$C_{20}H_{31}N_3O_{18}$	20	31	3	18
$C_{20}H_{32}N_3O_{18}$	20	32	3	18
$C_{20}H_{33}N_3O_{18}$	20	33	3	18
$C_{20}H_{31}N_3O_{19}$	20	31	3	19
$C_{20}H_{32}N_3O_{19}$	20	32	3	19
$C_{20}H_{33}N_3O_{19}$	20	33	3	19
$C_{20}H_{31}N_3O_{20}$	20	31	3	20
$C_{20}H_{33}N_3O_{20}$	20	33	3	20
$C_{20}H_{31}N_3O_{21}$	20	31	3	21
$C_{20}H_{30}N_4O_{14}$	20	30	4	14
$C_{20}H_{30}N_4O_{15}$	20	30	4	15
$C_{20}H_{34}N_4O_{15}$	20	34	4	15
$C_{20}H_{30}N_4O_{16}$	20	30	4	16
$C_{20}H_{34}N_4O_{16}$	20	34	4	16
$C_{20}H_{30}N_4O_{17}$	20	30	4	17
$C_{20}H_{34}N_4O_{17}$	20	34	4	17
$C_{20}H_{30}N_4O_{18}$	20	30	4	18
$C_{20}H_{34}N_4O_{18}$	20	34	4	18
$C_{20}H_{30}N_4O_{19}$	20	30	4	19
$C_{20}H_{34}N_4O_{19}$	20	34	4	19
$C_{20}H_{30}N_4O_{20}$	20	30	4	20
$C_{20}H_{34}N_4O_{20}$	20	34	4	20
$C_{20}H_{30}N_4O_{21}$	20	30	4	21

$C_{20}H_{30}N_4O_{22}$	20	30	4	22
$C_{21}H_{35}N_1O_7$	21	35	1	7
$C_{21}H_{35}N_1O_8$	21	35	1	8
$C_{21}H_{23}N_1O_{10}$	21	23	1	10
$C_{21}H_{40}N_1O_{14}$	21	40	1	14
$C_{21}H_{40}N_1O_{15}$	21	40	1	15
$C_{21}H_{42}N_1O_{15}$	21	42	1	15
$C_{22}H_{44}N_1O_{14}$	22	44	1	14
$C_{22}H_{30}N_1O_{15}$	22	30	1	15
$C_{24}H_{36}N_1O_9$	24	36	1	9
$C_{25}H_{32}N_2O_5$	25	32	2	5
$C_{25}H_{28}N_2O_{13}$	25	28	2	13
$C_{26}H_{34}N_2O_4$	26	34	2	4
$C_{26}H_{34}N_2O_5$	26	34	2	5
$C_{26}H_{47}N_3O_{20}$	26	47	3	20
$C_{26}H_{47}N_5O_{25}$	26	47	5	25
$C_{27}H_{34}N_2O_4$	27	34	2	4
$C_{27}H_{36}N_2O_4$	27	36	2	4
$C_{27}H_{36}N_2O_5$	27	36	2	5
$C_{27}H_{24}N_2O_6$	27	24	2	6
$C_{27}H_{44}N_6O_{16}$	27	44	6	16
$C_{28}H_{43}N_1O_{18}$	28	43	1	18
$C_{28}H_{38}N_2O_4$	28	38	2	4
$C_{28}H_{38}N_2O_5$	28	38	2	5
$C_{28}H_{44}N_2O_{16}$	28	44	2	16
$C_{28}H_{45}N_5O_{16}$	28	45	5	16
$C_{28}H_{45}N_5O_{17}$	28	45	5	17
$C_{28}H_{43}N_5O_{22}$	28	43	5	22
$C_{29}H_{44}N_2O_{22}$	29	44	2	22
$C_{29}H_{47}N_3O_{19}$	29	47	3	19
$C_{29}H_{45}N_3O_{20}$	29	45	3	20
$C_{29}H_{47}N_3O_{21}$	29	47	3	21
$C_{29}H_{48}N_4O_{18}$	29	48	4	18
$C_{29}H_{46}N_4O_{19}$	29	46	4	19
$C_{29}H_{46}N_4O_{20}$	29	46	4	20
$C_{29}H_{46}N_4O_{22}$	29	46	4	22
$C_{29}H_{46}N_4O_{23}$	29	46	4	23
$C_{29}H_{46}N_4O_{24}$	29	46	4	24
$C_{30}H_{47}N_1O_{18}$	30	47	1	18
$C_{30}H_{47}N_1O_{19}$	30	47	1	19
$C_{30}H_{48}N_2O_{18}$	30	48	2	18
$C_{30}H_{46}N_2O_{22}$	30	46	2	22
$C_{30}H_{48}N_2O_{23}$	30	48	2	23
$C_{30}H_{47}N_3O_{18}$	30	47	3	18

$C_{30}H_{49}N_3O_{18}$	30	49	3	18
$C_{30}H_{47}N_3O_{19}$	30	47	3	19
$C_{30}H_{49}N_3O_{20}$	30	49	3	20
$C_{30}H_{47}N_3O_{21}$	30	47	3	21
$C_{30}H_{49}N_3O_{22}$	30	49	3	22
$C_{30}H_{47}N_3O_{23}$	30	47	3	23
$C_{30}H_{47}N_3O_{24}$	30	47	3	24
$C_{30}H_{48}N_4O_{16}$	30	48	4	16
$C_{30}H_{48}N_4O_{17}$	30	48	4	17
$C_{30}H_{48}N_4O_{18}$	30	48	4	18
$C_{30}H_{48}N_4O_{19}$	30	48	4	19
$C_{30}H_{48}N_4O_{20}$	30	48	4	20
$C_{30}H_{48}N_4O_{21}$	30	48	4	21
$C_{30}H_{48}N_4O_{22}$	30	48	4	22
$C_{30}H_{48}N_4O_{23}$	30	48	4	23
$C_{30}H_{48}N_4O_{24}$	30	48	4	24
$C_{30}H_{49}N_5O_{20}$	30	49	5	20

[a]The molecular formulas were summarized from previous studies (Shen et al., 2022; Draper et al., 2015; Pullinen et al., 2020; Guo et al., 2022a; Shen et al., 2021; Xu et al., 2021a; DeVault and Ziemann, 2021; Guo et al., 2022b).

Table S4. Potential reactions in the precursor-product pair analysis.

NOCs	Reaction type	Specific reaction[a]	Variation of atoms
CHON+	Cond_N	Imination reaction	(+NH, −O)
		Intramolecular N-heterocyclic reaction	(+N, $-HO_2$)
	Hy_N	Hydrolysis reaction	(+O, −NH); ($+HO_2$, −N)
	De_N	Dehydration reaction	$-H_2O$
	Cond_hy_N	Mixed processes containing cond_N and hy_N	–
	Cond_de_N	Mixed processes containing cond_N and de_N	–
	Hy_de_N	Mixed processes containing hy_N and de_N	–
	Cond_hy_de_N	Mixed processes containing cond_N, hy_N and de_N	–
	Unknown_N	Unrecognized processes	–
CHN+	Cond_N	Intramolecular N-heterocyclic pathway	(+N, $-HO_2$)
	De_N	Dehydration reaction	$-H_2O$
	Cond_de_N	Mixed processes containing cond_N and de_N	–
	Unknown_N	Unrecognized processes	–
CHON–	Ox_N	Oxidation reaction	(−H, $+NO_2$)
	Hy_N	Hydrolysis reaction	(+H, $-NO_2$)
	Ox_hy_N	Mixed processes containing ox_N and hy_N	–
	Unknown_N	Unrecognized processes	–

[a]The reactions were summarized from previous publications (Abudumutailifu et al., 2024; Liu et al., 2023b; Jiang et al., 2023; Lv et al., 2022; Su et al., 2021; Laskin et al., 2014; Kames et al., 1993; Sun et al., 2024; Lian et al., 2020).

Table S5. Stress values from two-dimensional NMDS ordination for different NOCs across cities.

City	NOCs	Stress values
HEB	CHON+	0.037
	CHN+	0.039
	CHON−	0.066
BJ	CHON+	0.046
	CHN+	0.031
	CHON−	0.028
HZ	CHON+	0.113
	CHN+	0.067
	CHON−	0.077

Table S6. The number of compounds in each subgroup and the number and signal intensity fractions of each subgroup in ESI− mode across cities and periods.

City	Class	All period			Clean period			Haze period			Percentage
		Number	Number frac. (%)	Signal intensity frac. (%)	Number	Number frac. (%)	Signal intensity frac. (%)	Number	Number frac. (%)	Signal intensity frac. (%)	Percentage increase (%)[a]
HEB	**CHO+**	**528**	**28.2**	**10.3**	**524**	**28.2**	**13.0**	**516**	**28.3**	**9.5**	**240.7**
	$CHON_{1-3}$+	**713**	**38.1**	**21.5**	**702**	**37.8**	**23.7**	**686**	**37.6**	**20.8**	**307.4**
	$CHON_1$+	414	22.1	17.1	408	22.0	18.2	398	21.8	16.8	327.5
	$CHON_2$+	179	9.6	1.9	176	9.5	1.7	171	9.4	1.9	421.0
	$CHON_3$+	120	6.4	2.6	118	6.4	3.9	117	6.4	2.2	162.7
	CHN_{1-3}+	**633**	**33.8**	**68.2**	**630**	**33.9**	**63.3**	**622**	**34.1**	**69.6**	**410.3**
	CHN_1+	448	23.9	61.1	447	24.1	57.1	439	24.1	62.3	405.9
	CHN_2+	173	9.2	7.0	171	9.2	6.2	171	9.4	7.3	448.7
	CHN_3+	12	0.6	0.1	12	0.7	0.0	12	0.7	0.1	795.0
	Re-NOCs[b]	**1346**	**71.8**	**89.7**	**1332**	**71.8**	**87.0**	**1308**	**71.7**	**90.5**	**382.2**
	ALL ESI+	**1874**	**100.0**	**100.0**	**1856**	**100.0**	**100.0**	**1824**	**100.0**	**100.0**	**363.9**
BJ	**CHO+**	**533**	**28.1**	**23.6**	**530**	**28.1**	**26.5**	**524**	**28.5**	**20.4**	**43.0**
	$CHON_{1-3}$+	**727**	**38.4**	**31.6**	**725**	**38.4**	**34.8**	**694**	**37.7**	**28.1**	**49.9**
	$CHON_1$+	421	22.2	25.7	419	22.2	29.8	403	21.9	21.3	33.1
	$CHON_2$+	184	9.7	3.0	184	9.8	2.9	175	9.5	3.2	106.2
	$CHON_3$+	122	6.4	2.8	122	6.5	2.1	116	6.3	3.5	213.2
	CHN_{1-3}+	**634**	**33.5**	**44.9**	**631**	**33.5**	**38.7**	**621**	**33.8**	**51.6**	**148.0**
	CHN_1+	448	23.7	36.0	445	23.6	30.5	438	23.8	41.9	155.5
	CHN_2+	174	9.2	8.6	174	9.2	7.7	171	9.3	9.5	127.6
	CHN_3+	12	0.6	0.3	12	0.6	0.5	12	0.7	0.2	-9.5
	Re-NOCs	**1361**	**71.9**	**76.4**	**1356**	**71.9**	**73.5**	**1315**	**71.5**	**79.6**	**101.6**
	ALL ESI+	**1894**	**100.0**	**100.0**	**1886**	**100.0**	**100.0**	**1839**	**100.0**	**100.0**	**86.0**

	CHO+	**531**	**28.3**	**34.1**	**524**	**28.4**	**39.6**	**518**	**28.2**	**29.1**	**-18.1**
	$CHON_{1-3}$+	**715**	**38.1**	**35.0**	**700**	**37.9**	**36.1**	**697**	**37.9**	**34.0**	**4.5**
	$CHON_1$+	415	22.1	30.1	405	21.9	31.7	404	22.0	28.8	0.9
	$CHON_2$+	180	9.6	3.2	177	9.6	3.1	175	9.5	3.3	18.2
	$CHON_3$+	120	6.4	1.7	118	6.4	1.4	118	6.4	1.9	55.9
HZ	**CHN_{1-3}+**	**632**	**33.7**	**30.9**	**624**	**33.8**	**24.3**	**623**	**33.9**	**36.9**	**69.3**
	CHN_1+	445	23.7	23.7	437	23.7	17.8	438	23.8	29.0	81.5
	CHN_2+	175	9.3	6.9	175	9.5	6.1	173	9.4	7.6	38.6
	CHN_3+	12	0.6	0.3	12	0.7	0.4	12	0.7	0.3	-8.6
	Re-NOCs	**1347**	**71.7**	**65.9**	**1324**	**71.7**	**60.4**	**1320**	**71.8**	**70.9**	**30.5**
	ALL ESI+	**1878**	**100.0**	**100.0**	**1848**	**100.0**	**100.0**	**1838**	**100.0**	**100.0**	**11.3**

[a]It indicates the percentage increase in signal intensities for each group from clean to haze periods.

[b]Re-NOCs (Reduced NOCs) denote the sum of CHN_{1-3}+ and $CHON_{1-3}$+ compounds.

Table S7. The number, number fractions, and signal intensity fractions of each subgroup in ESI− mode in different cities and periods.

City	Class	All period			Clean period			Haze period			Percentage
		Number	Number frac. (%)	Signal intensity frac. (%)	Number	Number frac. (%)	Signal intensity frac. (%)	Number	Number frac. (%)	Signal intensity frac. (%)	Percentage increase (%)[a]
HEB	**CHO−**	**584**	**66.4**	**48.2**	**584**	**66.4**	**43.2**	**568**	**65.7**	**51.8**	**139.5**
	$CHON_{1-3}$−	**296**	**33.6**	**51.8**	**296**	**33.6**	**56.9**	**296**	**34.3**	**48.2**	**69.4**
	$CHON_1$−	190	21.6	48.0	190	21.6	52.4	190	22.0	45.0	71.4
	$CHON_2$−	72	8.2	2.1	72	8.2	3.1	72	8.3	1.5	-3.2
	$CHON_3$−	34	3.9	1.6	34	3.9	1.4	34	3.9	1.8	151.5
	ALL ESI−	**880**	**100.0**	**100.0**	**880**	**100.0**	**100.0**	**864**	**100.0**	**100.0**	**99.6**
BJ	**CHO−**	**589**	**66.3**	**54.7**	**586**	**66.1**	**52.7**	**575**	**66.0**	**58.5**	**15.3**
	$CHON_{1-3}$−	**300**	**33.8**	**45.3**	**300**	**33.9**	**47.3**	**297**	**34.1**	**41.5**	**-9.1**
	$CHON_1$−	193	21.7	37.9	193	21.8	39.0	191	21.9	35.8	-4.7
	$CHON_2$−	73	8.2	5.9	73	8.2	6.7	72	8.3	4.4	-31.8
	$CHON_3$−	34	3.8	1.5	34	3.9	1.6	34	3.9	1.2	-21.9
	ALL ESI−	**889**	**100.0**	**100.0**	**886**	**100.0**	**100.0**	**872**	**100.0**	**100.0**	**3.8**
HZ	**CHO−**	**593**	**66.3**	**67.7**	**587**	**66.2**	**69.3**	**589**	**66.2**	**66.1**	**-5.8**
	$CHON_{1-3}$−	**301**	**33.7**	**32.3**	**300**	**33.8**	**30.7**	**301**	**33.8**	**33.9**	**8.9**
	$CHON_1$−	194	21.7	24.2	194	21.9	22.7	194	21.8	25.7	11.7
	$CHON_2$−	73	8.2	7.2	72	8.1	7.0	73	8.2	7.3	3.3
	$CHON_3$−	34	3.8	0.9	34	3.8	1.0	34	3.8	0.8	-14.1
	ALL ESI−	**894**	**100.0**	**100.0**	**887**	**100.0**	**100.0**	**890**	**100.0**	**100.0**	**-1.3**

[a]It represents the percentage increase in signal intensity for each group from clean to haze periods.

Table S8. Signal intensity fractions of each subgroup of CHON+ and CHON− compounds in different cities and periods.

Mode	City	Period	Aliphatics-derived Re_NOCs (%)	Heterocyclics-derived Re_NOCs (%)	Aromatics-derived Re_NOCs (%)	Isoprene-derived Ox_NOCs (%)	Monoterpenes-derived Ox_NOCs (%)	Aromatics-derived Ox_NOCs (%)	Aliphatics-derived Ox_NOCs (%)	Unclassified Ox_NOCs (%)
CHON+	HEB	All	3.3	2.8	72.9	0.1	0.1	14.6	5.2	1.0
		Clean	7.1	7.6	59.1	0.1	0.3	17.7	7.6	0.6
		Haze	2.0	1.2	77.7	0.1	0.0	13.5	4.4	1.1
	BJ	All	20.8	20.8	33.0	0.3	0.5	14.7	9.6	0.4
		Clean	22.4	24.2	30.8	0.3	0.6	11.5	9.8	0.4
		Haze	18.7	16.1	35.9	0.2	0.4	19.0	9.3	0.3
	HZ	All	27.5	22.7	23.0	0.5	0.7	11.8	13.6	0.2
		Clean	27.3	24.4	24.9	0.5	0.5	10.1	12.1	0.2
		Haze	27.7	21.1	21.3	0.5	0.9	13.3	15.0	0.2
CHON−	HEB	All	0.4	0.0	3.6	1.3	0.3	90.3	2.3	1.8
		Clean	0.3	0.0	2.9	0.7	0.2	91.0	1.9	3.0
		Haze	0.4	0.0	4.2	1.8	0.4	89.7	2.6	0.9
	BJ	All	0.1	0.0	4.5	1.3	0.5	85.7	4.4	3.5
		Clean	0.1	0.0	4.4	1.3	0.5	84.9	5.0	3.8
		Haze	0.1	0.0	4.8	1.2	0.6	87.3	3.2	2.7
	HZ	All	0.3	0.0	9.9	1.0	1.7	71.6	4.4	11.1
		Clean	0.1	0.0	8.8	1.1	1.6	69.7	6.2	12.6
		Haze	0.5	0.0	11.0	0.8	1.8	73.4	2.8	9.7

Table S9. The number, number fractions, and signal intensity fractions of each subgroup of CHN+ compounds in different cities and periods.

City	Class	All period			Clean period			Haze period			Percentage
		Number	Number frac. (%)	Signal intensity frac. (%)	Number	Number frac. (%)	Signal intensity frac. (%)	Number	Number frac. (%)	Signal intensity frac. (%)	Percentage increase (%)[a]
HEB	Aliphatic CHN+	98	7.2	15.5	97	7.6	15.4	97	7.1	15.6	373.7
	Monoaromatic CHN+	311	51.9	49.1	309	49.5	49.1	305	52.6	49.0	442.3
	Polyaromatic CHN+	224	40.9	35.4	224	42.9	35.6	220	40.3	35.4	379.8
	All	633	100.0	100.0	630	100.0	100.0	622	100.0	100.0	410.3
BJ	Aliphatic CHN+	99	14.3	15.6	99	11.6	15.7	98	16.5	15.8	251.7
	Monoaromatic CHN+	311	48.4	49.1	310	54.9	49.1	304	43.2	49.0	95.4
	Polyaromatic CHN+	224	37.3	35.3	222	33.5	35.2	219	40.3	35.3	198.2
	All	**634**	**100.0**	**100.0**	**631**	**100.0**	**100.0**	**621**	**100.0**	**100.0**	**148.0**
HZ	Aliphatic CHN+	99	35.5	15.7	99	32.6	15.9	98	37.2	15.7	93.2
	Monoaromatic CHN+	311	50.9	49.2	308	54.5	49.4	307	48.7	49.3	51.2
	Polyaromatic CHN+	222	13.7	35.1	217	12.9	34.8	218	14.1	35.0	85.3
	All	**632**	**100.0**	**100.0**	**624**	**100.0**	**100.0**	**623**	**100.0**	**100.0**	**69.3**

[a]It indicates the percentage increase in signal intensities of each group from clean to haze periods.

Table S10. The peak intensity-weighted average MF_w, MM_w, elemental ratios, DBE_w, Xc_w, AI_{modw}, and OS_{Cw} for different NOCs in different cities and periods.

City	Periods	Subgroups	MF_w	MM_w	O/C_w	H/C_w	N/C_w	O/N_w	DBE_w	Xc_w	AI_{modw}	OSc_w
HEB	All period	CHON+	$C_{11.49}H_{14.96}O_{1.97}N_{1.33}$	203.1	0.2	1.3	0.1	1.4	5.7	2.6	0.4	-0.9
		CHN+	$C_{13.19}H_{13.27}N_{1.11}$	187.1	–[a]	1.1	0.1	–	8.1	2.7	0.6	-1.1
		CHON−	$C_{7.84}H_{8.65}O_{3.86}N_{1.1}$	180.0	0.5	1.1	0.2	3.6	5.1	2.4	0.6	0.0
	Clean period	CHON+	$C_{13.51}H_{20.47}O_{2.18}N_{1.4}$	237.3	0.2	1.4	0.1	1.5	5.0	2.5	0.3	-1.1
		CHN+	$C_{13.4}H_{13.01}N_{1.1}$	189.3	–	1.0	0.1	–	8.5	2.7	0.6	-1.0
		CHON−	$C_{8.14}H_{9.26}O_{3.87}N_{1.1}$	184.4	0.5	1.1	0.2	3.6	5.1	2.4	0.6	-0.1
	Haze period	CHON+	$C_{10.8}H_{13.07}O_{1.9}N_{1.3}$	191.3	0.2	1.2	0.1	1.4	5.9	2.7	0.5	-0.8
		CHN+	$C_{13.13}H_{13.34}N_{1.11}$	186.5	–	1.1	0.1	–	8.0	2.7	0.6	-1.1
		CHON−	$C_{7.59}H_{8.14}O_{3.85}N_{1.1}$	176.3	0.5	1.1	0.2	3.7	5.1	2.4	0.6	0.0
BJ	All period	CHON+	$C_{16.48}H_{29.49}O_{1.98}N_{1.27}$	277.0	0.2	1.7	0.1	1.5	3.4	2.0	0.2	-1.4
		CHN+	$C_{13.8}H_{15.15}N_{1.21}$	197.8	–	1.1	0.1	–	7.8	2.6	0.5	-1.1
		CHON−	$C_{8.75}H_{10.58}O_{4.01}N_{1.2}$	196.6	0.5	1.1	0.2	3.5	5.1	2.4	0.6	-0.1
	Clean period	CHON+	$C_{17.21}H_{31.44}O_{1.76}N_{1.2}$	283.3	0.1	1.8	0.1	1.4	3.1	1.8	0.1	-1.5
		CHN+	$C_{13.84}H_{15.7}N_{1.22}$	199.0	–	1.1	0.1	–	7.6	2.6	0.5	-1.1
		CHON−	$C_{8.94}H_{11}O_{4.01}N_{1.21}$	199.5	0.5	1.1	0.2	3.5	5.0	2.4	0.5	-0.1
	Haze period	CHON+	$C_{15.51}H_{26.89}O_{2.27}N_{1.36}$	268.6	0.2	1.7	0.1	1.5	3.8	2.2	0.2	-1.3
		CHN+	$C_{13.77}H_{14.7}N_{1.19}$	196.7	–	1.1	0.1	–	8.0	2.6	0.5	-1.1
		CHON−	$C_{8.35}H_{9.64}O_4N_{1.17}$	190.3	0.5	1.1	0.2	3.6	5.1	2.4	0.6	0.0

HZ	All period	CHON+	$C_{19.04}H_{36.31}O_{1.81}N_{1.19}$	310.6	0.1	1.9	0.1	1.5	2.5	1.7	0.1	-1.7
		CHN+	$C_{13.09}H_{19.15}N_{1.25}$	193.8	–	1.5	0.1	–	5.1	2.1	0.4	-1.5
		CHON−	$C_{9.64}H_{12.79}O_{4.05}N_{1.28}$	211.3	0.5	1.2	0.2	3.4	4.9	2.2	0.5	-0.2
	Clean period	CHON+	$C_{19.14}H_{36.49}O_{1.71}N_{1.16}$	310.0	0.1	1.9	0.1	1.5	2.5	1.6	0.1	-1.7
		CHN+	$C_{12.09}H_{16.8}N_{1.28}$	180.0	–	1.4	0.1	–	5.3	2.2	0.4	-1.4
		CHON−	$C_{10.2}H_{14.28}O_{4.16}N_{1.29}$	221.5	0.5	1.2	0.2	3.4	4.7	2.2	0.5	-0.3
	Haze period	CHON+	$C_{18.95}H_{36.14}O_{1.91}N_{1.21}$	311.3	0.1	1.9	0.1	1.6	2.5	1.8	0.1	-1.7
		CHN+	$C_{13.68}H_{20.54}N_{1.22}$	202.0	–	1.5	0.1	–	5.0	2.1	0.3	-1.5
		CHON−	$C_{9.13}H_{11.43}O_{3.95}N_{1.27}$	201.9	0.5	1.1	0.2	3.4	5.0	2.2	0.6	-0.1

[a]The symbol "–" indicates no data.

Table S11. The number, number fractions, and signal intensity fractions of CHON+ compounds formed through different processes.

City	Class	All period			Clean period			Haze period		
		Number	Number frac. (%)	Signal intensity frac. (%)	Number	Number frac. (%)	Signal intensity frac. (%)	Number	Number frac. (%)	Signal intensity frac. (%)
HEB	Cond_N	181	25.4	33.6	179	25.5	32.5	176	25.7	33.6
	Hy_N	62	8.7	3.8	60	8.6	4.1	62	9.0	3.6
	De_N	16	2.2	0.6	16	2.3	1.6	16	2.3	0.3
	Cond_hy_N	206	28.9	38.1	205	29.2	31.2	194	28.3	40.6
	Cond_de_N	46	6.5	2.2	44	6.3	5.0	42	6.1	1.3
	Hy_de_N	4	0.6	0.1	4	0.6	0.3	3	0.4	0.0
	Cond_hy_de_N	54	7.6	4.4	52	7.4	2.6	51	7.4	4.9
	[a]Mix_N	**310**	**43.5**	**44.8**	**305**	**43.5**	**39.0**	**290**	**42.3**	**46.8**
	Unknown_N	144	20.2	17.2	142	20.2	22.8	142	20.7	15.6
	All	**713**	**100.0**	**100.0**	**702**	**100.0**	**100.0**	**686**	**100.0**	**100.0**
BJ	Cond_N	186	25.6	34.3	186	25.7	37.7	179	25.8	29.7
	Hy_N	66	9.1	4.1	66	9.1	4.1	60	8.7	4.1
	De_N	17	2.3	0.6	17	2.3	0.6	16	2.3	0.7
	Cond_hy_N	209	28.8	18.0	208	28.7	16.6	200	28.8	19.8
	Cond_de_N	48	6.6	16.4	48	6.6	17.8	44	6.3	14.5
	Hy_de_N	4	0.6	0.4	4	0.6	0.6	4	0.6	0.2
	Cond_hy_de_N	55	7.6	2.1	55	7.6	1.5	53	7.6	2.9
	[a]Mix_N	**316**	**43.5**	**36.9**	**315**	**43.5**	**36.5**	**301**	**43.4**	**37.4**
	Unknown_N	142	19.5	24.1	141	19.5	21.1	138	19.9	28.1
	All	**727**	**100.0**	**100.0**	**725**	**100.0**	**100.0**	**694**	**100.0**	**100.0**

HZ	Cond_N	181	25.3	31.9	179	25.6	33.8	177	25.4	29.9
	Hy_N	63	8.8	5.7	62	8.9	5.5	63	9.0	5.9
	De_N	16	2.2	0.7	14	2.0	0.4	16	2.3	0.7
	Cond_hy_N	209	29.2	17.2	203	29.0	18.4	202	29.0	16.1
	Cond_de_N	45	6.3	19.9	44	6.3	19.3	44	6.3	20.6
	Hy_de_N	3	0.4	0.6	3	0.4	0.8	3	0.4	0.5
	Cond_hy_de_N	54	7.6	1.4	53	7.6	1.1	52	7.5	1.8
	[a]Mix_N	**311**	**43.5**	**39.2**	**303**	**43.3**	**39.5**	**301**	**43.2**	**38.9**
	Unknown_N	144	20.1	22.6	142	20.3	20.8	140	20.1	24.5
	All	**715**	**100.0**	**100.0**	**700**	**100.0**	**100.0**	**697**	**100.0**	**100.0**

[a] Mix_N process includes cond_hy_N, cond_de_N, hy_de_N, and cond_hy_de_N pathways.

Table S12. The number, number fractions and signal intensity fractions of CHN+ compounds formed through different processes.

City	Class	All period			Clean period			Haze period		
		Number	Number frac. (%)	Signal intensity frac. (%)	Number	Number frac. (%)	Signal intensity frac. (%)	Number	Number frac. (%)	Signal intensity frac. (%)
HEB	Cond_N	134	27.4	21.2	129	22.7	20.5	134	28.6	21.5
	De_N	39	1.8	6.2	38	1.1	6.0	39	2.0	6.3
	Cond_de_N	172	33.8	27.2	172	37.7	27.3	165	32.8	26.5
	Unknown_N	288	37.0	45.5	291	38.5	46.2	284	36.7	45.7
	All	**633**	**100.0**	**100.0**	**630**	**100.0**	**100.0**	**622**	**100.0**	**100.0**
BJ	Cond_N	133	20.4	21.0	133	20.4	21.1	127	20.3	20.5
	De_N	39	5.7	6.2	39	5.4	6.2	38	6.0	6.1
	Cond_de_N	172	34.8	27.1	172	38.5	27.3	169	31.8	27.2
	Unknown_N	290	39.1	45.7	287	35.7	45.5	287	41.9	46.2
	All	**634**	**100.0**	**100.0**	**631**	**100.0**	**100.0**	**621**	**100.0**	**100.0**
HZ	Cond_N	134	12.6	21.2	132	13.1	21.2	134	12.8	21.5
	De_N	39	10.3	6.2	38	9.5	6.1	38	10.7	6.1
	Cond_de_N	174	38.0	27.5	174	47.7	27.9	161	31.7	25.8
	Unknown_N	285	39.1	45.1	280	29.7	44.9	290	44.8	46.6
	All	**632**	**100.0**	**100.0**	**624**	**100.0**	**100.0**	**623**	**100.0**	**100.0**

Table S13. The number, number fractions and signal intensity fractions of CHON− compounds formed through different processes.

City	Class	All period			Clean period			Haze period		
		Number	Number frac. (%)	Signal intensity frac. (%)	Number	Number frac. (%)	Signal intensity frac. (%)	Number	Number frac. (%)	Signal intensity frac. (%)
HEB	Ox_N	104	10.8	35.1	104	12.3	35.1	104	9.6	35.1
	Hy_N	12	1.7	4.1	12	1.2	4.1	12	2.2	4.1
	Ox_hy_N	35	66.4	11.8	35	63.7	11.8	35	68.6	11.8
	Unknown_N	145	21.1	49.0	145	22.9	49.0	145	19.6	49.0
	All	**296**	**100.0**	**100.0**	**296**	**100.0**	**100.0**	**296**	**100.0**	**100.0**
BJ	Ox_N	107	15.2	35.7	107	15.9	35.7	105	13.6	35.4
	Hy_N	12	1.3	4.0	12	1.5	4.0	11	0.8	3.7
	Ox_hy_N	35	57.0	11.7	35	53.9	11.7	35	63.7	11.8
	Unknown_N	146	26.6	48.7	146	28.7	48.7	146	21.9	49.2
	All	**300**	**100.0**	**100.0**	**300**	**100.0**	**100.0**	**297**	**100.0**	**100.0**
HZ	Ox_N	107	18.1	35.6	107	15.8	35.7	102	20.1	33.9
	Hy_N	12	0.6	4.0	12	0.6	4.0	12	0.7	4.0
	Ox_hy_N	35	46.1	11.6	35	45.0	11.7	35	47.0	11.6
	Unknown_N	147	35.2	48.8	146	38.6	48.7	152	32.2	50.5
	All	**301**	**100.0**	**100.0**	**300**	**100.0**	**100.0**	**301**	**100.0**	**100.0**

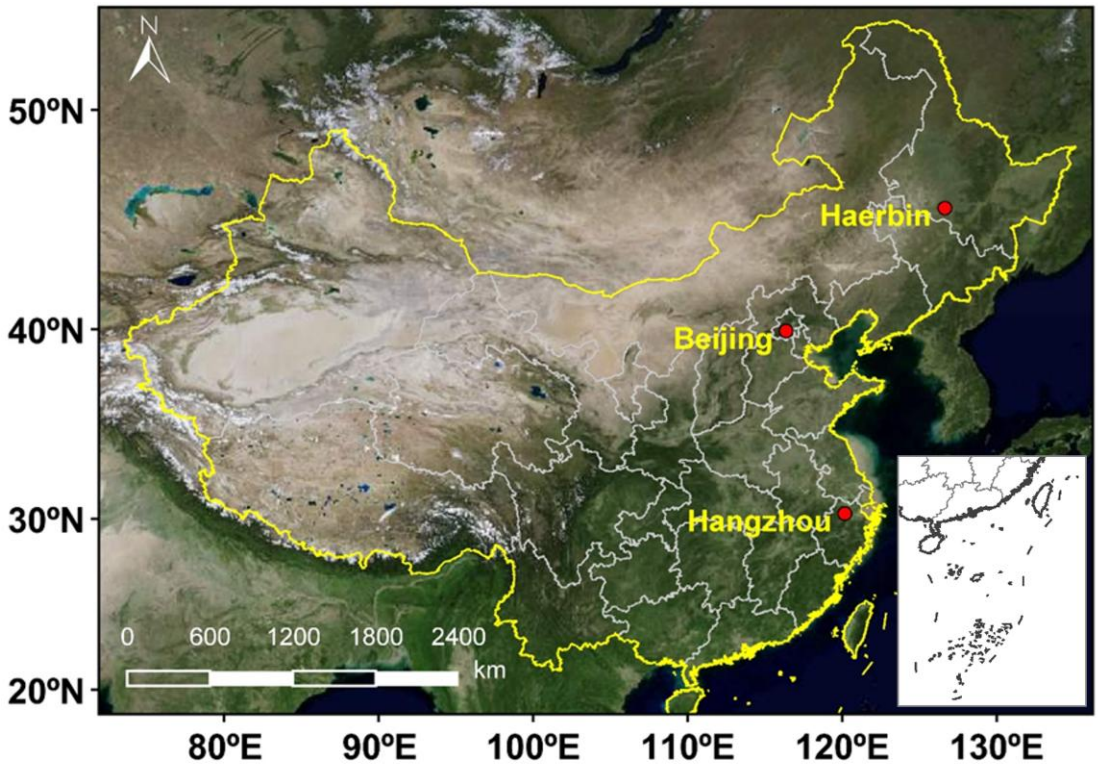

Figure S1. The location of the $PM_{2.5}$ sampling sites in HEB, BJ, and HZ, respectively. The map is derived from ©MeteoInfoMap (version 3.6.2) (Chinese Academy of Meteorological Sciences, China). The figure may contain a territory that is disputed according to the United Nations.

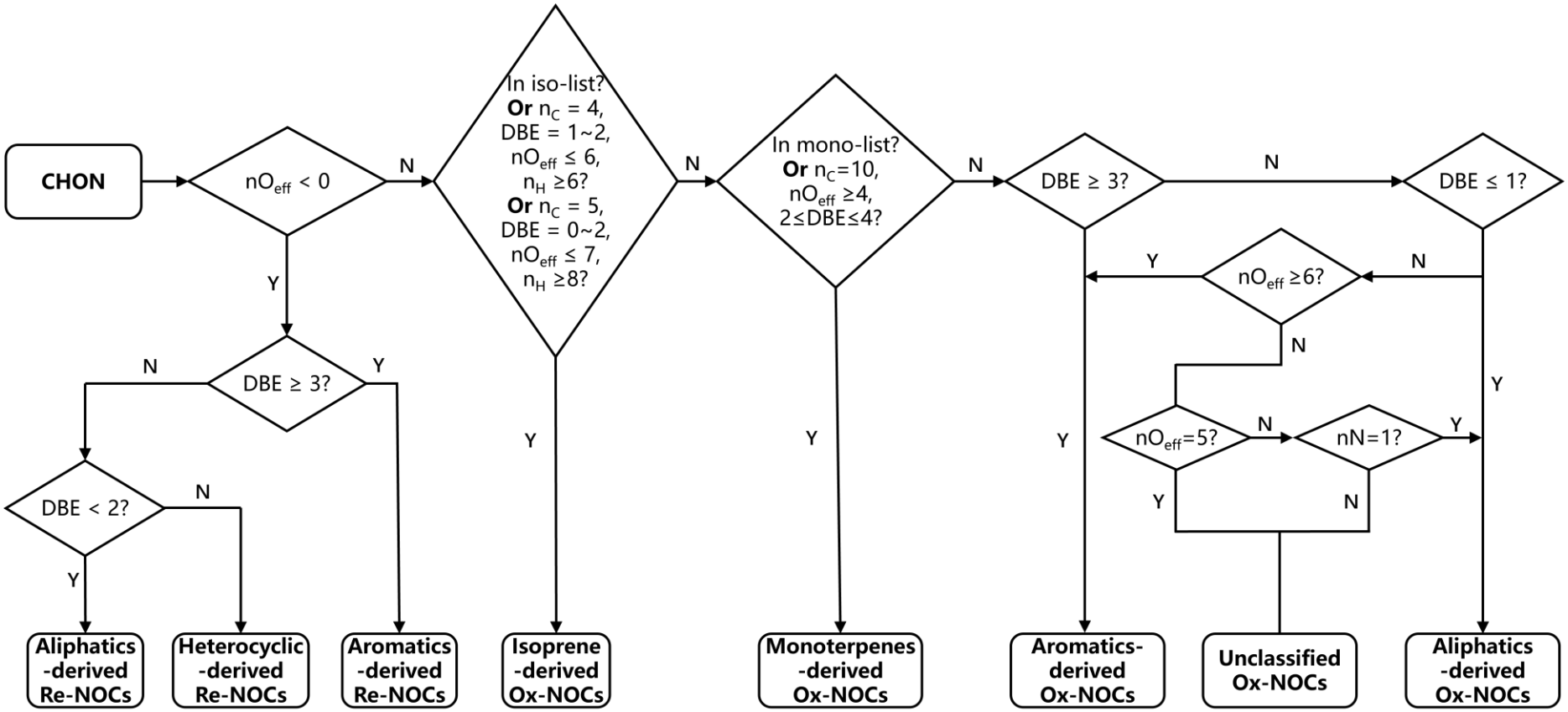

Figure S2. Workflow for identifying the potential precursors of CHON compounds. The symbol nO_{eff}, n_C, n_H, and n_N represent the number of effective oxygen, carbon, hydrogen, and nitrogen atoms in each CHON molecular formula, respectively. The symbols 'Y' and 'N' represent 'yes' and 'no,' respectively.

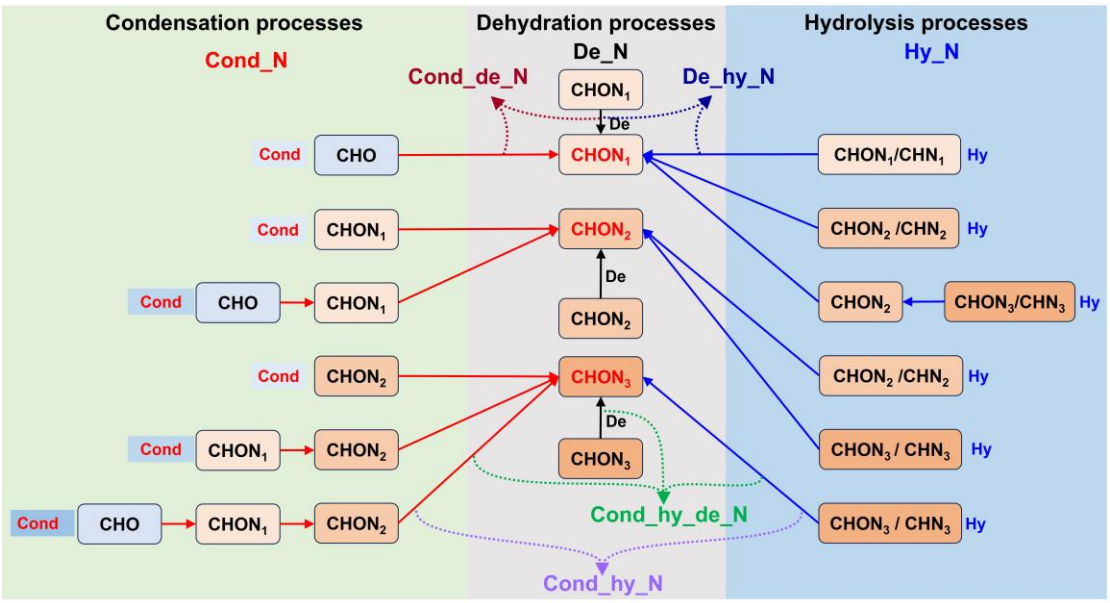

Figure S3. Schematic diagram for identifying the different formation processes of CHON+ compounds.

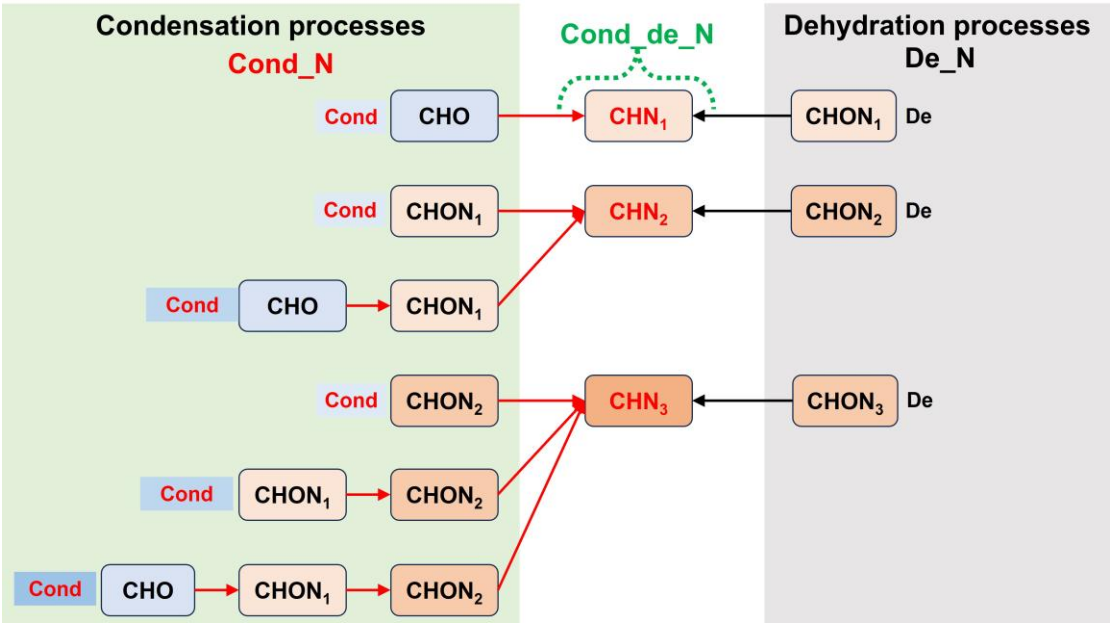

Figure S4. Schematic diagram for identifying the different formation processes of CHN+ compounds.

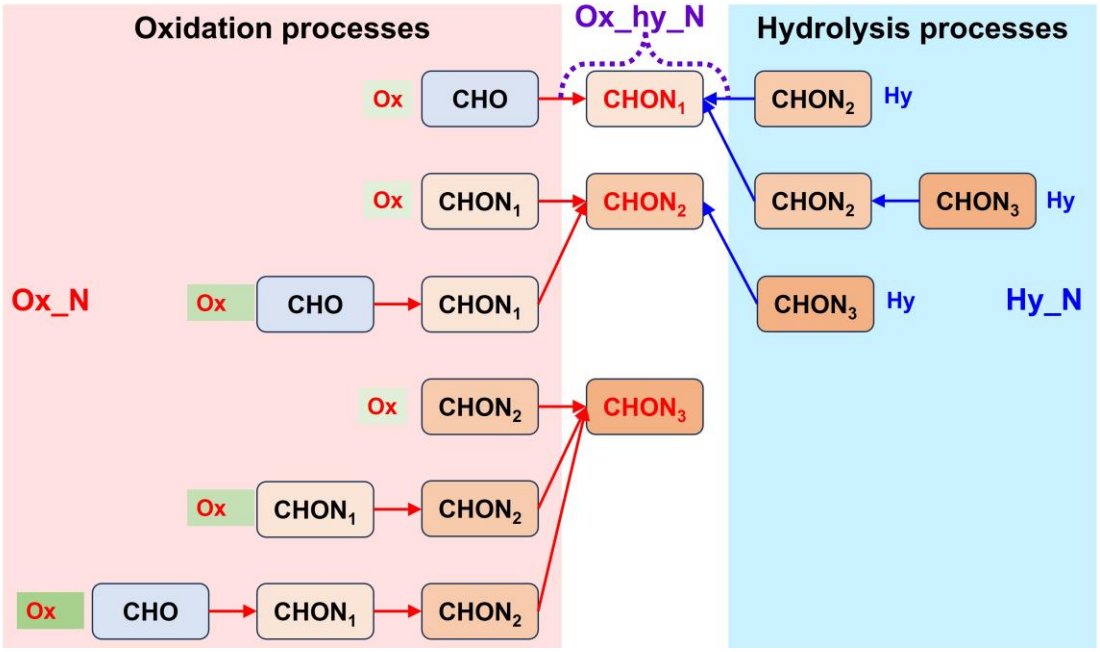

Figure S5. Schematic diagram for identifying the different formation processes of CHON− compounds.

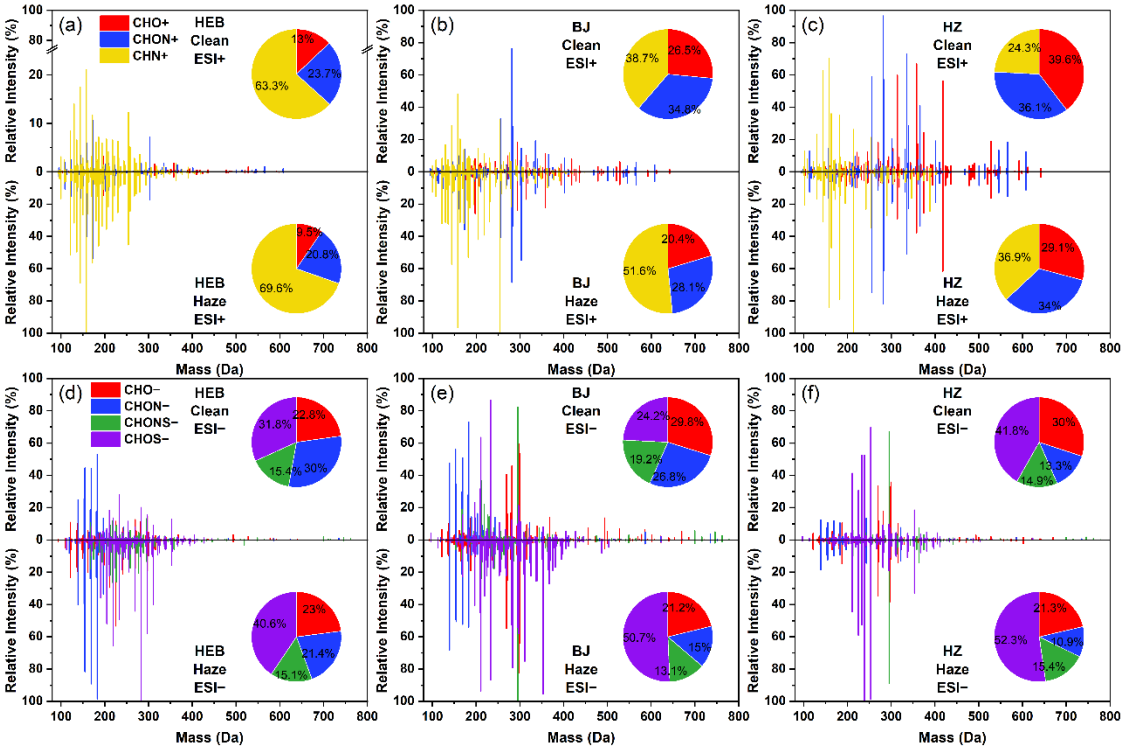

Figure S6. Reconstructed mass spectrum distributions of detected species in $PM_{2.5}$ for (**a–c**) ESI+ and (**d–f**) ESI− modes in different cities. The vertical axis represents the relative signal intensity of each compound compared to that of the compound with the highest peak intensity. The pie charts show the signal intensity fractions of classified compounds among all species detected in $PM_{2.5}$ during different periods.

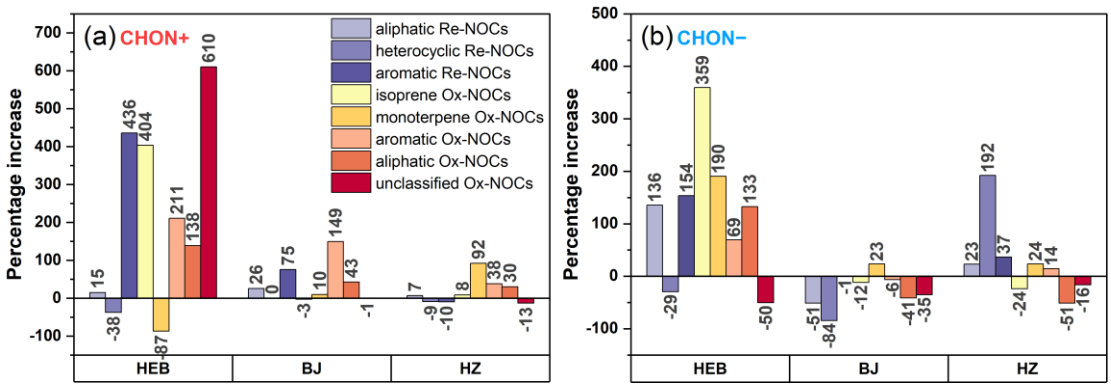

Figure S7. Percentage variations in the signal intensities of each subgroup of (**a**) CHON+ and (**b**) CHON− compounds from haze to clean periods in different cities.

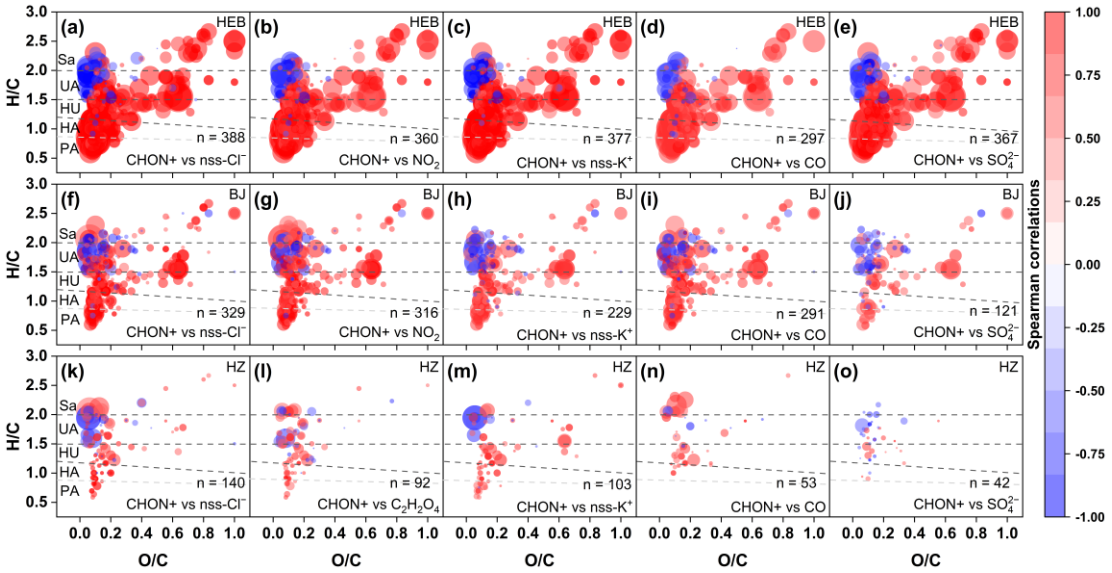

Figure S8. Spearman rank correlation coefficients (with $P < 0.01$ in HEB and $P < 0.05$ in BJ and HZ) of individual CHON+ molecules with selected parameters in (**a–e**) HEB, (**f–j**) BJ, and (**k–o**) HZ. The color scale indicates the Spearman correlations between the intensities of individual CHON+ molecules and each parameter. The symbol *n* in the bottom-right corner of each panel indicates the number of molecular formulas significantly correlated with the variables (e.g., nss-Cl^-, nss-K^-, and CO). The subgroups of compounds in the panels include polycyclic aromatic-like (PA), highly aromatic-like (HA), highly unsaturated-like (HU), unsaturated aliphatic-like (UA), and saturated-like (Sa) compounds.

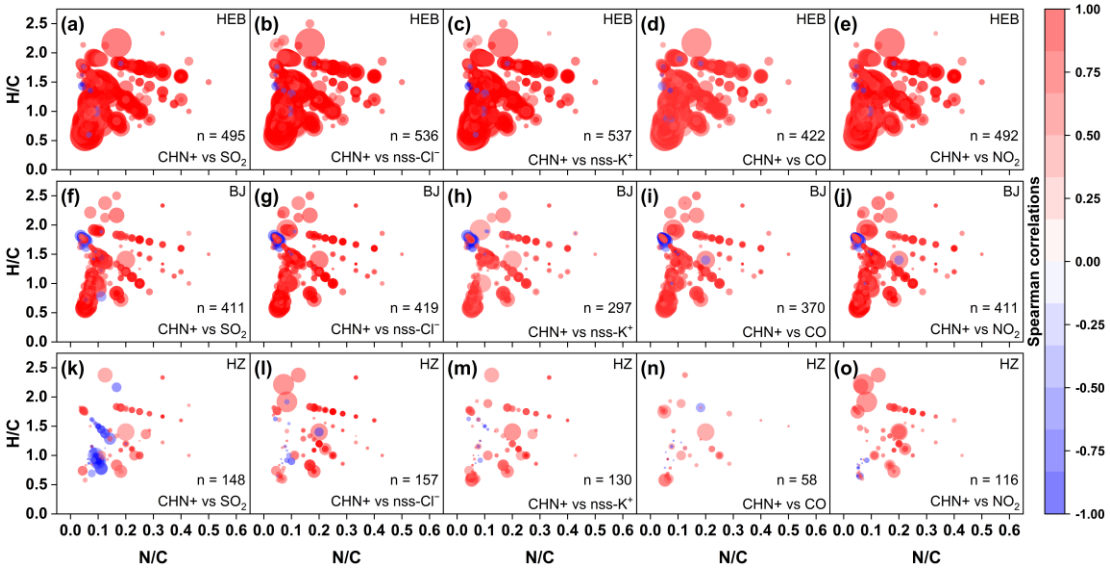

Figure S9. Spearman rank correlation coefficients (with $P < 0.01$ in HEB and $P < 0.05$ in BJ and HZ) of individual CHN+ molecules with selected parameters in (**a–e**) HEB, (**f–j**) BJ, and (**k–o**) HZ. The color scale indicates the Spearman correlations between the intensities of individual CHN+ molecules and each parameter. The symbol *n* in the bottom-right corner of each panel represents the number of molecular formulas significantly correlated with the variables (e.g., SO_2, nss-Cl^-, nss-K^-, CO, and NO_2).

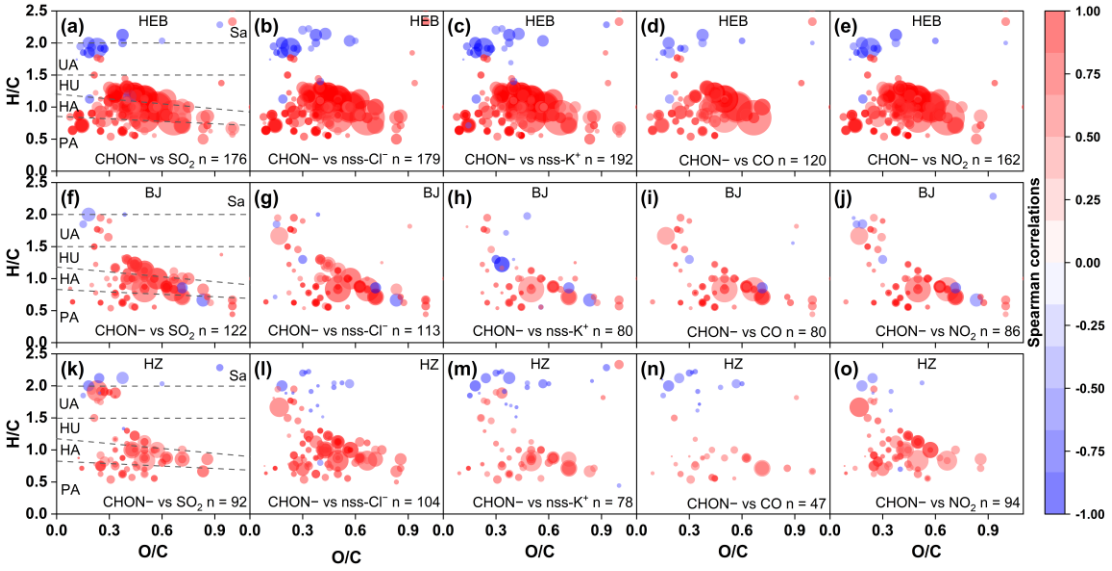

Figure S10. Spearman rank correlation coefficients (with $P < 0.01$ in HEB and $P < 0.05$ in BJ and HZ) of individual CHON− molecules with selected parameters in (**a–e**) HEB, (**f–j**) BJ, and (**k–o**) HZ. The color scale indicates the Spearman correlations between the intensities of individual CHON− molecules and each parameter. The symbol *n* in the bottom-right corner of each panel represents the number of molecular formulas significantly correlated with the variables (e.g., SO_2, nss-Cl^-, nss-K^-, CO, and NO_2). The subgroups of compounds in the panels include polycyclic aromatic-like (PA), highly aromatic-like (HA), highly unsaturated-like (HU), unsaturated aliphatic-like (UA), and saturated-like (Sa) compounds.

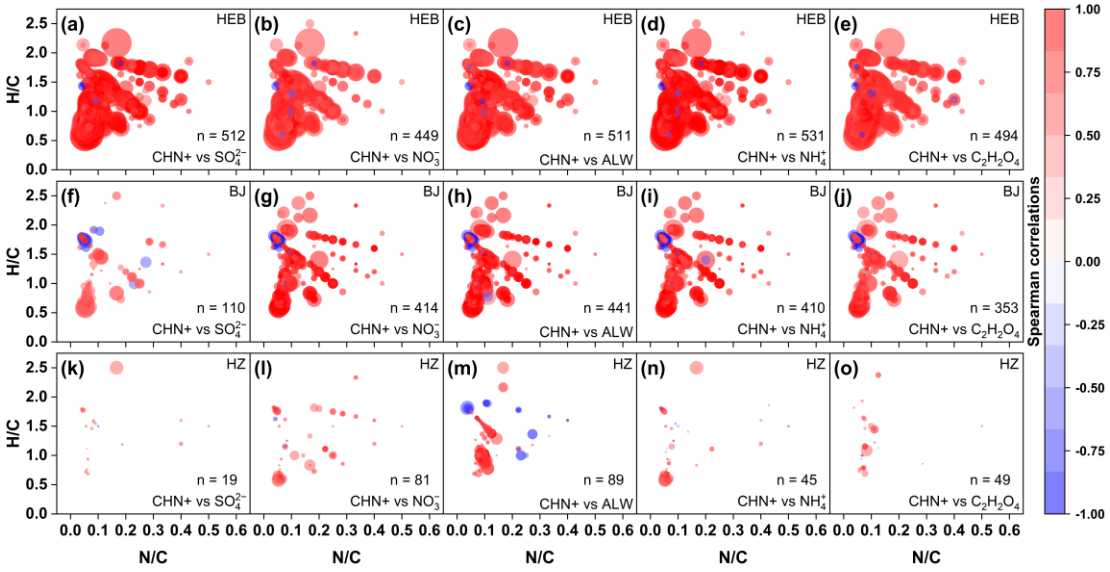

Figure S11. Spearman rank correlation coefficients (with $P < 0.01$ in HEB and $P < 0.05$ in BJ and HZ) of individual CHN+ molecules with selected parameters in (**a–e**) HEB, (**f–j**) BJ, and (**k–o**) HZ. The color scale indicates the Spearman correlations between the intensities of individual CHN+ molecules and each parameter. The symbol *n* in the bottom-right corner of each panel indicates the number of molecular formulas significantly correlated with the variables (e.g., SO_4^{2+}, NO_3^-, ALW, NH_4^+, and $C_2H_4O_4$).

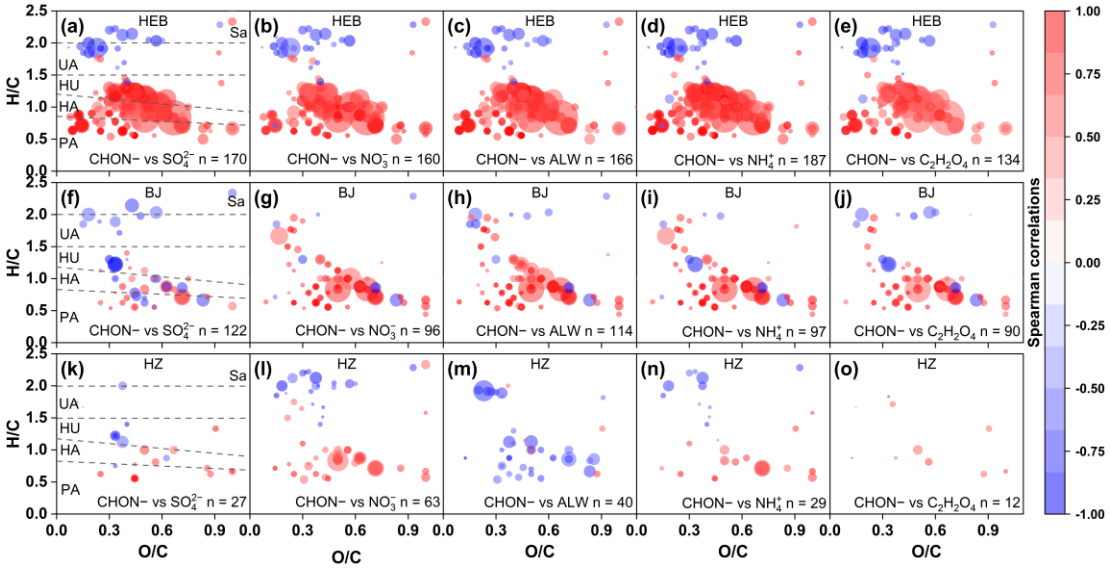

Figure S12. Spearman rank correlation coefficients (with $P < 0.01$ in HEB and $P < 0.05$ in BJ and HZ) of individual CHON− molecules with selected parameters in (**a–e**) HEB, (**f–j**) BJ, and (**k–o**) HZ. The color scale indicates the Spearman correlations between the intensities of individual CHON− molecules and each parameter. The symbol *n* in the bottom-right corner of each panel represents the number of molecular formulas significantly correlated with the variables (e.g., SO_4^{2+}, NO_3^-, ALW, NH_4^+, and $C_2H_4O_4$). The subgroups of compounds in the panels include polycyclic aromatic-like (PA), highly aromatic-like (HA), highly unsaturated-like (HU), unsaturated aliphatic-like (UA), and saturated-like (Sa) compounds.

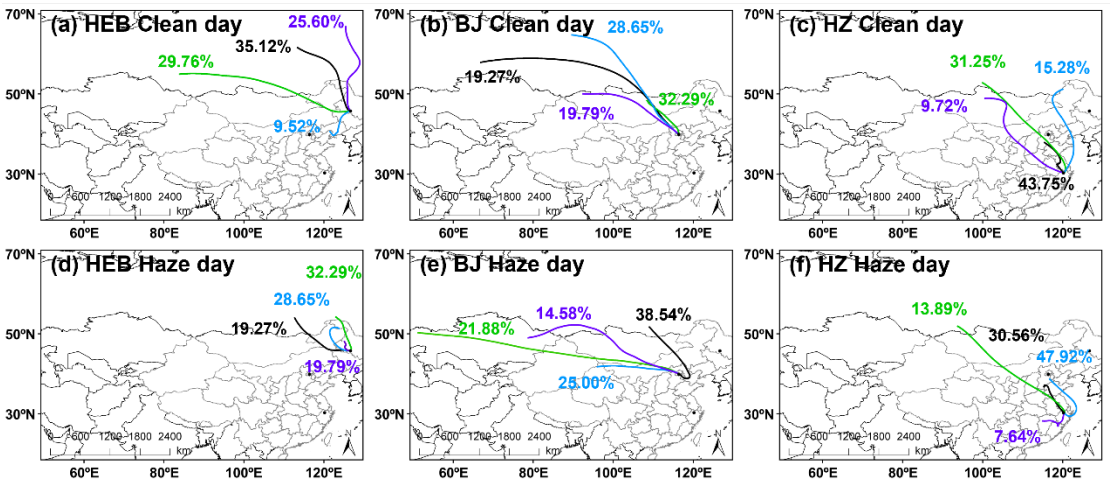

Figure S13. Three-day (72 h) back trajectories illustrating the major air mass transported to the study sites during the (**a–c**) clean and (**d–f**) haze periods. The map is derived from ©MeteoInfoMap (version 3.6.2) (Chinese Academy of Meteorological Sciences, China).

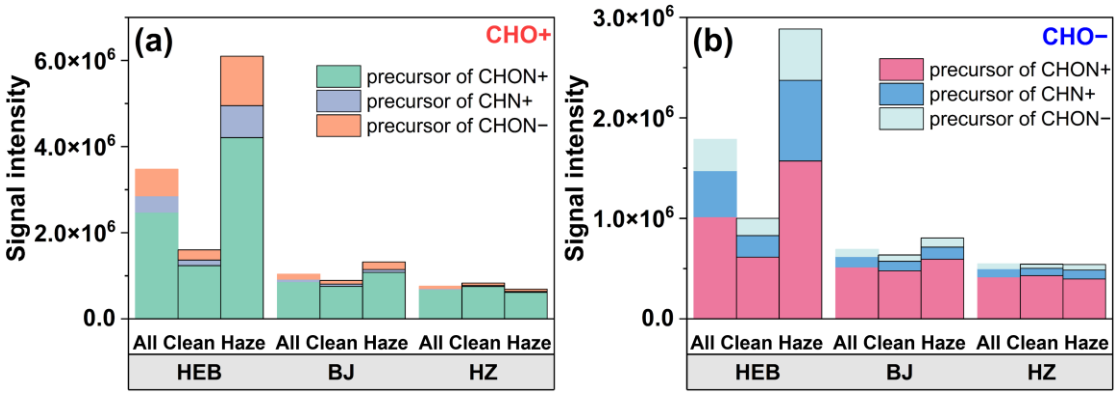

Figure S14. Average signal intensity distributions of (**a**) CHO+ and (**b**) CHO− precursors of NOCs in $PM_{2.5}$ samples collected from different cities during winter.

REFERENCES

Abudumutailifu, M., Shang, X., Wang, L., Zhang, M., Kang, H., Chen, Y., Li, L., Ju, R., Li, B., Ouyang, H., Tang, X., Li, C., Wang, L., Wang, X., George, C., Rudich, Y., Zhang, R., and Chen, J.: Unveiling the Molecular Characteristics, Origins, and Formation Mechanism of Reduced Nitrogen Organic Compounds in the Urban Atmosphere of Shanghai Using a Versatile Aerosol Concentration Enrichment System, Environ. Sci. Technol., 10.1021/acs.est.3c04071, 2024.

Bae, E., Yeo, I. J., Jeong, B., Shin, Y., Shin, K.-H., and Kim, S.: Study of Double Bond Equivalents and the Numbers of Carbon and Oxygen Atom Distribution of Dissolved Organic Matter with Negative-Mode FT-ICR MS, Anal. Chem., 83, 4193-4199, 10.1021/ac200464q, 2011.

Boyd, C. M., Sanchez, J., Xu, L., Eugene, A. J., Nah, T., Tuet, W. Y., Guzman, M. I., and Ng, N. L.: Secondary organic aerosol formation from the β-pinene+NO_3 system: effect of humidity and peroxy radical fate, Atmos. Chem. Phys., 15, 7497-7522, 10.5194/acp-15-7497-2015, 2015.

Darer, A. I., Cole-Filipiak, N. C., O'Connor, A. E., and Elrod, M. J.: Formation and Stability of Atmospherically Relevant Isoprene-Derived Organosulfates and Organonitrates, Environ. Sci. Technol., 45, 1895-1902, 10.1021/es103797z, 2011.

DeVault, M. P. and Ziemann, P. J.: Gas- and Particle-Phase Products and Their Mechanisms of Formation from the Reaction of Δ-3-Carene with NO_3 Radicals, The Journal of Physical Chemistry A, 125, 10207-10222, 10.1021/acs.jpca.1c07763, 2021.

Draper, D. C., Farmer, D. K., Desyaterik, Y., and Fry, J. L.: A qualitative comparison of secondary organic aerosol yields and composition from ozonolysis of monoterpenes at varying concentrations of NO_2, Atmos. Chem. Phys., 15, 12267-12281, 10.5194/acp-15-12267-2015, 2015.

Guo, Y., Shen, H., Pullinen, I., Luo, H., Kang, S., Vereecken, L., Fuchs, H., Hallquist, M., Acir, I. H., Tillmann, R., Rohrer, F., Wildt, J., Kiendler-Scharr, A., Wahner, A., Zhao, D., and Mentel, T. F.: Identification of highly oxygenated organic molecules and their role in aerosol formation in the reaction of limonene with nitrate radical, Atmos. Chem. Phys., 22, 11323-11346, 10.5194/acp-22-11323-2022, 2022a.

Guo, Y., Yan, C., Liu, Y., Qiao, X., Zheng, F., Zhang, Y., Zhou, Y., Li, C., Fan, X., Lin, Z., Feng, Z., Zhang, Y., Zheng, P., Tian, L., Nie, W., Wang, Z., Huang, D., Daellenbach, K. R., Yao, L., Dada, L., Bianchi, F., Jiang, J., Liu, Y., Kerminen, V. M., and Kulmala, M.: Seasonal variation in oxygenated organic molecules in urban Beijing and their contribution to secondary organic aerosol, Atmos. Chem. Phys., 22, 10077-10097, 10.5194/acp-22-10077-2022, 2022b.

Jiang, H., Cai, J., Feng, X., Chen, Y., Wang, L., Jiang, B., Liao, Y., Li, J., Zhang, G., Mu, Y., and Chen, J.: Aqueous-Phase Reactions of Anthropogenic Emissions Lead to the High Chemodiversity of Atmospheric Nitrogen-Containing Compounds during the Haze Event, Environ. Sci. Technol., 57, 16500-16511, 10.1021/acs.est.3c06648, 2023.

Kames, J., Schurath, U., Flocke, F., and Volz-Thomas, A.: Preparation of organic nitrates from alcohols and N_2O_5 for species identification in atmospheric samples,

Journal of Atmospheric Chemistry, 16, 349-359, 10.1007/BF01032630, 1993.

Kroll, J. H., Donahue, N. M., Jimenez, J. L., Kessler, S. H., Canagaratna, M. R., Wilson, K. R., Altieri, K. E., Mazzoleni, L. R., Wozniak, A. S., Bluhm, H., Mysak, E. R., Smith, J. D., Kolb, C. E., and Worsnop, D. R.: Carbon oxidation state as a metric for describing the chemistry of atmospheric organic aerosol, Nat. Chem., 3, 133-139, https://doi.org/10.1038/nchem.948, 2011.

Kruve, A., Kaupmees, K., Liigand, J., and Leito, I.: Negative Electrospray Ionization via Deprotonation: Predicting the Ionization Efficiency, Anal. Chem., 86, 4822-4830, 10.1021/ac404066v, 2014.

Kuehnbaum, N. L. and Britz-McKibbin, P.: New Advances in Separation Science for Metabolomics: Resolving Chemical Diversity in a Post-Genomic Era, Chem. Rev., 113, 2437-2468, 10.1021/cr300484s, 2013.

Laskin, J., Laskin, A., Roach, P. J., Slysz, G. W., Anderson, G. A., Nizkorodov, S. A., Bones, D. L., and Nguyen, L. Q.: High-Resolution Desorption Electrospray Ionization Mass Spectrometry for Chemical Characterization of Organic Aerosols, Anal. Chem., 82, 2048-2058, 10.1021/ac902801f, 2010.

Laskin, J., Laskin, A., Nizkorodov, S. A., Roach, P., Eckert, P., Gilles, M. K., Wang, B., Lee, H. J., and Hu, Q.: Molecular Selectivity of Brown Carbon Chromophores, Environ. Sci. Technol., 48, 12047-12055, https://doi.org/10.1021/es503432r, 2014.

Lechtenfeld, O. J., Kattner, G., Flerus, R., McCallister, S. L., Schmitt-Kopplin, P., and Koch, B. P.: Molecular transformation and degradation of refractory dissolved organic matter in the Atlantic and Southern Ocean, Geochim. Cosmochim. Acta,

126, 321-337, https://doi.org/10.1016/j.gca.2013.11.009, 2014.

Leito, I., Herodes, K., Huopolainen, M., Virro, K., Künnapas, A., Kruve, A., and Tanner, R.: Towards the electrospray ionization mass spectrometry ionization efficiency scale of organic compounds, Rapid Commun. Mass Spectrom., 22, 379-384, https://doi.org/10.1002/rcm.3371, 2008.

Lian, L., Yan, S., Zhou, H., and Song, W.: Overview of the Phototransformation of Wastewater Effluents by High-Resolution Mass Spectrometry, Environ. Sci. Technol., 54, 1816-1826, 10.1021/acs.est.9b04669, 2020.

Liu, X., Wang, H., Wang, F., Lv, S., Wu, C., Zhao, Y., Zhang, S., Liu, S., Xu, X., Lei, Y., and Wang, G.: Secondary Formation of Atmospheric Brown Carbon in China Haze: Implication for an Enhancing Role of Ammonia, Environ. Sci. Technol., 57, 11163-11172, 10.1021/acs.est.3c03948, 2023a.

Liu, Z., Zhu, B., Zhu, C., Ruan, T., Li, J., Chen, H., Li, Q., Wang, X., Wang, L., Mu, Y., Collett, J., George, C., Wang, Y., Wang, X., Su, J., Yu, S., Mellouki, A., Chen, J., and Jiang, G.: Abundant nitrogenous secondary organic aerosol formation accelerated by cloud processing, iScience, 26, 108317, https://doi.org/10.1016/j.isci.2023.108317, 2023b.

Lv, S., Wang, F., Wu, C., Chen, Y., Liu, S., Zhang, S., Li, D., Du, W., Zhang, F., Wang, H., Huang, C., Fu, Q., Duan, Y., and Wang, G.: Gas-to-Aerosol Phase Partitioning of Atmospheric Water-Soluble Organic Compounds at a Rural Site in China: An Enhancing Effect of NH_3 on SOA Formation, Environ. Sci. Technol., 56, 3915-3924, 10.1021/acs.est.1c06855, 2022.

Ma, Y. J., Xu, Y., Yang, T., Xiao, H. W., and Xiao, H. Y.: Measurement report: Characteristics of nitrogen-containing organics in $PM_{2.5}$ in Ürümqi, northwestern China – differential impacts of combustion of fresh and aged biomass materials, Atmos. Chem. Phys., 24, 4331-4346, 10.5194/acp-24-4331-2024, 2024.

Ng, N. L., Kwan, A. J., Surratt, J. D., Chan, A. W. H., Chhabra, P. S., Sorooshian, A., Pye, H. O. T., Crounse, J. D., Wennberg, P. O., Flagan, R. C., and Seinfeld, J. H.: Secondary organic aerosol (SOA) formation from reaction of isoprene with nitrate radicals (NO_3), Atmos. Chem. Phys., 8, 4117-4140, 10.5194/acp-8-4117-2008, 2008.

Ni, T., Li, P., Han, B., Bai, Z., Ding, X., Wang, Q., Huo, J., and Lu, B.: Spatial and Temporal Variation of Chemical Composition and Mass Closure of Ambient PM_{10} in Tianjin, China, Aerosol and Air Quality Research, 13, 1832-1846, 10.4209/aaqr.2012.10.0283, 2013.

Nie, W., Yan, C., Huang, D. D., Wang, Z., Liu, Y., Qiao, X., Guo, Y., Tian, L., Zheng, P., Xu, Z., Li, Y., Xu, Z., Qi, X., Sun, P., Wang, J., Zheng, F., Li, X., Yin, R., Dallenbach, K. R., Bianchi, F., Petäjä, T., Zhang, Y., Wang, M., Schervish, M., Wang, S., Qiao, L., Wang, Q., Zhou, M., Wang, H., Yu, C., Yao, D., Guo, H., Ye, P., Lee, S., Li, Y. J., Liu, Y., Chi, X., Kerminen, V.-M., Ehn, M., Donahue, N. M., Wang, T., Huang, C., Kulmala, M., Worsnop, D., Jiang, J., and Ding, A.: Secondary organic aerosol formed by condensing anthropogenic vapours over China's megacities, Nature Geoscience, 15, 255-261, 10.1038/s41561-022-00922-5, 2022.

Núñez, O. and Paolo, L.: Applications and uses of formic acid in liquid

chromatography-mass spectrometry analysis, in: Advances in Chemistry Research, edited by: Taylor, J. C., Nova Science Publishers, 71-86, 2014.

Praplan, A. P., Hegyi-Gaeggeler, K., Barmet, P., Pfaffenberger, L., Dommen, J., and Baltensperger, U.: Online measurements of water-soluble organic acids in the gas and aerosol phase from the photooxidation of 1,3,5-trimethylbenzene, Atmos. Chem. Phys., 14, 8665-8677, 10.5194/acp-14-8665-2014, 2014.

Pullinen, I., Schmitt, S., Kang, S., Sarrafzadeh, M., Schlag, P., Andres, S., Kleist, E., Mentel, T. F., Rohrer, F., Springer, M., Tillmann, R., Wildt, J., Wu, C., Zhao, D., Wahner, A., and Kiendler-Scharr, A.: Impact of NO_x on secondary organic aerosol (SOA) formation from α-pinene and β-pinene photooxidation: the role of highly oxygenated organic nitrates, Atmos. Chem. Phys., 20, 10125-10147, 10.5194/acp-20-10125-2020, 2020.

Schmidt, A.-C., Herzschuh, R., Matysik, F.-M., and Engewald, W.: Investigation of the ionisation and fragmentation behaviour of different nitroaromatic compounds occurring as polar metabolites of explosives using electrospray ionisation tandem mass spectrometry, Rapid Commun. Mass Spectrom., 20, 2293-2302, https://doi.org/10.1002/rcm.2591, 2006.

Seidel, M., Beck, M., Riedel, T., Waska, H., Suryaputra, I. G. N. A., Schnetger, B., Niggemann, J., Simon, M., and Dittmar, T.: Biogeochemistry of dissolved organic matter in an anoxic intertidal creek bank, Geochim. Cosmochim. Acta, 140, 418-434, https://doi.org/10.1016/j.gca.2014.05.038, 2014.

Shen, H., Vereecken, L., Kang, S., Pullinen, I., Fuchs, H., Zhao, D., and Mentel, T. F.:

Unexpected significance of a minor reaction pathway in daytime formation of biogenic highly oxygenated organic compounds, Science Advances, 8, eabp8702, doi:10.1126/sciadv.abp8702, 2022.

Shen, H., Zhao, D., Pullinen, I., Kang, S., Vereecken, L., Fuchs, H., Acir, I.-H., Tillmann, R., Rohrer, F., Wildt, J., Kiendler-Scharr, A., Wahner, A., and Mentel, T. F.: Highly Oxygenated Organic Nitrates Formed from NO_3 Radical-Initiated Oxidation of β-Pinene, Environ. Sci. Technol., 10.1021/acs.est.1c03978, 2021.

Song, J., Li, M., Jiang, B., Wei, S., Fan, X., and Peng, P. a.: Molecular Characterization of Water-Soluble Humic like Substances in Smoke Particles Emitted from Combustion of Biomass Materials and Coal Using Ultrahigh-Resolution Electrospray Ionization Fourier Transform Ion Cyclotron Resonance Mass Spectrometry, Environ. Sci. Technol., 52, 2575-2585, https://doi.org/10.1021/acs.est.7b06126, 2018.

Su, S., Xie, Q., Lang, Y., Cao, D., Xu, Y., Chen, J., Chen, S., Hu, W., Qi, Y., Pan, X., Sun, Y., Wang, Z., Liu, C.-Q., Jiang, G., and Fu, P.: High Molecular Diversity of Organic Nitrogen in Urban Snow in North China, Environ. Sci. Technol., 55, 4344-4356, https://dx.doi.org/10.1021/acs.est.0c06851, 2021.

Sun, W., Hu, X., Fu, Y., Zhang, G., Zhu, Y., Wang, X., Yan, C., Xue, L., Meng, H., Jiang, B., Liao, Y., Wang, X., Peng, P., and Bi, X.: Different formation pathways of nitrogen-containing organic compounds in aerosols and fog water in northern China, Atmos. Chem. Phys., 24, 6987-6999, 10.5194/acp-24-6987-2024, 2024.

Tian, L., Huang, D. D., Li, Y. J., Yan, C., Nie, W., Wang, Z., Wang, Q., Qiao, L., Zhou,

M., Zhu, S., Liu, Y., Guo, Y., Qiao, X., Zheng, P., Jing, S. a., Lou, S., Wang, H., and Huang, C.: Enigma of Urban Gaseous Oxygenated Organic Molecules: Precursor Type, Role of NO_x, and Degree of Oxygenation, Environ. Sci. Technol., 57, 64-75, 10.1021/acs.est.2c05047, 2023.

Ungeheuer, F., van Pinxteren, D., and Vogel, A. L.: Identification and source attribution of organic compounds in ultrafine particles near Frankfurt International Airport, Atmos. Chem. Phys., 21, 3763-3775, 10.5194/acp-21-3763-2021, 2021.

Wang, D., Shen, Z., Yang, X., Huang, S., Luo, Y., Bai, G., and Cao, J.: Insight into the Role of NH_3/NH_4^+ and NO_x/NO_3^- in the Formation of Nitrogen-Containing Brown Carbon in Chinese Megacities, Environ. Sci. Technol., 58, 4281-4290, 10.1021/acs.est.3c10374, 2024.

Wang, K., Huang, R.-J., Brueggemand, M., Zhang, Y., Yang, L., Ni, H., Guo, J., Wang, M., Han, J., Bilde, M., Glasius, M., and Hoffmann, T.: Urban organic aerosol composition in eastern China differs from north to south: molecular insight from a liquid chromatography-mass spectrometry (Orbitrap) study, Atmos. Chem. Phys., 21, 9089-9104, https://doi.org/10.5194/acp-21-9089-2021, 2021a.

Wang, Y., Zhao, Y., Li, Z., Li, C., Yan, N., and Xiao, H.: Importance of Hydroxyl Radical Chemistry in Isoprene Suppression of Particle Formation from α-Pinene Ozonolysis, ACS Earth Space Chem., 5, 487-499, https://doi.org/10.1021/acsearthspacechem.0c00294, 2021b.

Wang, Y., Zhao, Y., Wang, Y., Yu, J. Z., Shao, J., Liu, P., Zhu, W., Cheng, Z., Li, Z., Yan, N., and Xiao, H.: Organosulfates in atmospheric aerosols in Shanghai, China:

seasonal and interannual variability, origin, and formation mechanisms, Atmos. Chem. Phys., 21, 2959-2980, 10.5194/acp-21-2959-2021, 2021c.

Wu, R., Vereecken, L., Tsiligiannis, E., Kang, S., Albrecht, S. R., Hantschke, L., Zhao, D., Novelli, A., Fuchs, H., Tillmann, R., Hohaus, T., Carlsson, P. T. M., Shenolikar, J., Bernard, F., Crowley, J. N., Fry, J. L., Brownwood, B., Thornton, J. A., Brown, S. S., Kiendler-Scharr, A., Wahner, A., Hallquist, M., and Mentel, T. F.: Molecular composition and volatility of multi-generation products formed from isoprene oxidation by nitrate radical, Atmos. Chem. Phys., 21, 10799-10824, 10.5194/acp-21-10799-2021, 2021.

Xu, L., Yang, Z., Tsona, N. T., Wang, X., George, C., and Du, L.: Anthropogenic-Biogenic Interactions at Night: Enhanced Formation of Secondary Aerosols and Particulate Nitrogen- and Sulfur-Containing Organics from β-Pinene Oxidation, Environ. Sci. Technol., 10.1021/acs.est.0c07879, 2021a.

Xu, Y., Dong, X. N., He, C., Wu, D. S., Xiao, H. W., and Xiao, H. Y.: Mist cannon trucks can exacerbate the formation of water-soluble organic aerosol and $PM_{2.5}$ pollution in the road environment, Atmos. Chem. Phys., 23, 6775-6788, https://doi.org/10.5194/acp-23-6775-2023, 2023.

Xu, Z. N., Nie, W., Liu, Y. L., Sun, P., Huang, D. D., Yan, C., Krechmer, J., Ye, P. L., Xu, Z., Qi, X. M., Zhu, C. J., Li, Y. Y., Wang, T. Y., Wang, L., Huang, X., Tang, R. Z., Guo, S., Xiu, G. L., Fu, Q. Y., Worsnop, D., Chi, X. G., and Ding, A. J.: Multifunctional Products of Isoprene Oxidation in Polluted Atmosphere and Their Contribution to SOA, Geophys. Res. Lett., 48, e2020GL089276,

https://doi.org/10.1029/2020GL089276, 2021b.

Yassine, M. M., Harir, M., Dabek-Zlotorzynska, E., and Schmitt-Kopplin, P.: Structural characterization of organic aerosol using Fourier transform ion cyclotron resonance mass spectrometry: Aromaticity equivalent approach, Rapid Commun. Mass Spectrom., 28, 2445-2454, https://doi.org/10.1002/rcm.7038, 2014.

Zhang, M., Cai, D., Lin, J., Liu, Z., Li, M., Wang, Y., and Chen, J.: Molecular characterization of atmospheric organic aerosols in typical megacities in China, npj Climate and Atmospheric Science, 7, 230, 10.1038/s41612-024-00784-1, 2024.

Zhao, D., Pullinen, I., Fuchs, H., Schrade, S., Wu, R., Acir, I. H., Tillmann, R., Rohrer, F., Wildt, J., Guo, Y., Kiendler-Scharr, A., Wahner, A., Kang, S., Vereecken, L., and Mentel, T. F.: Highly oxygenated organic molecule (HOM) formation in the isoprene oxidation by NO_3 radical, Atmos. Chem. Phys., 21, 9681-9704, 10.5194/acp-21-9681-2021, 2021.

Zhong, S., Chen, S., Deng, J., Fan, Y., Zhang, Q., Xie, Q., Qi, Y., Hu, W., Wu, L., Li, X., Pavuluri, C. M., Zhu, J., Wang, X., Liu, D., Pan, X., Sun, Y., Wang, Z., Xu, Y., Tong, H., Su, H., Cheng, Y., Kawamura, K., and Fu, P.: Impact of biogenic secondary organic aerosol (SOA) loading on the molecular composition of wintertime $PM_{2.5}$ in urban Tianjin: an insight from Fourier transform ion cyclotron resonance mass spectrometry, Atmos. Chem. Phys., 23, 2061-2077, https://doi.org/10.5194/acp-23-2061-2023, 2023.

Zou, C., Cao, T., Li, M., Song, J., Jiang, B., Jia, W., Li, J., Ding, X., Yu, Z., Zhang, G., and Peng, P.: Measurement report: Changes in light absorption and molecular

composition of water-soluble humic-like substances during a winter haze bloom-decay process in Guangzhou, China, Atmos. Chem. Phys., 23, 963-979, https://doi.org/10.5194/acp-23-963-2023, 2023.